UNIVERSIDADE DE LISBOA
FACULDADE DE CIÊNCIAS
DEPARTAMENTO DE FISICA


# Links between defective endocytosis and mitochondria

Katarzyna Więciorek

**Mestrado Integrado em Engenharia Biomédica e Biofísica**

Biofísica Médica e Fisiologia de Sistemas

Dissertação orientada por:

**Alexandre Andrade, Prof.**

**Ira Milosevic, Ph.D.**

**2017**

Universidade de Lisboa

Faculdade de Ciências

**Katarzyna Więciorek**

Dissertation

**Links between defective endocytosis and mitochondria**

Lisbon, 2017

Supervisor: Prof. Alexandre Andrade

Auxiliary supervisor: Ira Milosevic, Ph.D.

## ABSTRACT

Several links between endocytosis and the maintenance of mitochondrial structure and function have been reported, yet they are poorly understood. Endocytic proteins, such as membrane curvature sensor endophilin B, GTPases dynamin-2 and dynamin-related protein-1 (Drp1), are necessary for proper mitochondrial function. Moreover, inhibitors of clathrin mediated endocytosis, endosidin9 and tyrosine kinase inhibitor tyrphostin A23, uncouple mitochondrial oxidative phosphorylation.

The main goal of this work was to explore effects of impaired endocytosis using the mammalian model without key endocytic proteins, endophilin-A or phosphatase synaptojanin-1, on mitochondrial function. Statistical analysis of Next Generation Sequencing (NGS) data indicates that knock-out of endophilin-A, or synaptojanin-1, leads to a downregulation of transcript levels of genes encoding mitochondrial proteins. Mitochondrial malfunction was identified based on the following criteria: reduced membrane potential, decreased oxygen consumption rate and elevated reactive oxygen species production. The glycolytic pathway has also been affected in both mutants. Moreover, increased lysosomal mass and diminished proteolytic activity were observed, which are characteristic of lysosomal dysfunction.

Functional iron deficiency was detected in endophilin-A triple knock-out, which most likely contributes to observed mitochondrial malfunction since iron is a crucial cofactor in various biological processes, such as oxygen transport, cellular respiration and mTORC1 signalling. Notably, mTOR pathway regulates iron metabolism and homeostasis: PI3K/AKT/mTOR pathway was found significantly affected by knock-out of endophilin-A (activities of AKT and mTOR are reduced). Abnormal activity of PI3K/AKT/mTOR pathway may have multiple consequences since mTOR signalling coordinates key aspects of metabolism at both the cellular and organismal level. Proper mTOR activity is also necessary for regulation of protein synthesis, autophagy and critical neurological processes. Overall, endophilin-A and synaptojanin-1 are necessary for proper mitochondrial and lysosomal function, and lack of endophilin-A leads to functional iron deficiency and significantly decreased activity of PI3K/AKT/mTOR pathway.

Keywords: endocytosis, mitochondria, synaptojanin-1, endophilin-A

Universidade de Lisboa

Faculdade de Ciências

**Katarzyna Więciorek**

Dissertação

**Ligações entre endocitose defeituosa e mitocôndrias**

Lisbon, 2017

Supervisor: Prof. Alexandre Andrade

Supervisor auxiliar: Ira Milosevic, Ph.D.

## SUMARIO

Os mecanismos de endocitose e de manutenção da estrutura e função mitocondriais têm um aspecto comum: diversas proteínas, como as endofilinas B e as GTPases dinamina-2 e proteína relacionada com a dinamina (DRP1) são necessárias para que os mitocôndrios funcionem apropriadamente. Além disso, os inibidores de endocitose mediada pela clatrina endosidin9 e tyrphostinA23 desacoplam a fosforilação oxidativa mitocondrial.

O objectivo principal deste trabalho foi verificar como é que deficiências em endocitose, pelo *knock-out* de proteínas endocíticas endofilinas A ou sinaptojanina-1, afectam a função mitochondrial. A análise estatística de resultados de *Next Generation Sequencing* indicam que o *knock-out* de endofilinas A ou sinaptojanina-1 resulta numa repressão generalizada dos níveis transcricionais de genes que codificam proteínas mitocondriais. A disfunção mitochondrial foi caracterizada com base nos critérios seguintes: potencial de membrana reduzido, menor velocidade de consumo de oxigénio, e aumento na produção de espécies reactivas de oxigénio. A via da glicólise também foi afectada pela deficiência em endocitose. Além disso, foi observado um aumento da massa lisossomal e uma diminuição da capacidade proteolítica do lisossoma, o que configura um quadro de disfunção lisossomal.

Foi detectada uma robusta deficiência funcional de ferro nos *knock-outs* triplos das endofilinas A, o que muito provavelmente contribui para a disfunção mitochondrial observada, dado que o ferro é um cofactor crucial em vários processos biológicos, como respiração cellular e sinalização mTORC1. Além disso, a via mTOR regula a homeostase do ferro.

Conforme esperado, a via PI3K/AKT/mTOR foi significativamente afectada pelo *knock-out* de endofilinas A, particularmente com uma redução notável nas activades de AKT e mTOR. Esta actividade anormal pode ter consequências sérias porque a sinalização pelo mTOR coordena o metabolismo tanto ao nível celular como sistémico. A actividade apropriada de mTOR é tambem necessária para a regulação da síntese de proteínas, autofagia e processos neurológicos críticos, como desenvolvimento neuronal. Globalmente, as endofilinas A e a sinaptojanina-1 são necessárias para a função apropriada de mitocôndrios e lisossomas, e a falta de endofilinas A resulta em deficiência funcional de ferro e numa redução significativa da actividade da via PI3K/Akt/mTOR.

Palavras-chave: endocitose, mitocôndrio, sinaptojanina, endofilinas A

**Acknowledgements**

I would like to express my very great appreciation to the Dean, professor José Artur Martinho Simões. I would like to offer my special thanks to the professor Alexandre Andrade, my thesis supervisor, for his guidance and useful critiques of this research work. I am particularly grateful for the support given by staff of Institute of Biophysics and Biomedical Engineering during my studies in Lisbon and work in Göttingen as well. I would like to thank the Erasmus Programme for providing foreign exchange option and scholarship.

I would like to express my very great gratitude to Ira Milosevic, Ph. D. as she decided to give me a chance to enrich my knowledge and develop my skills participating in traineeship at the European Neuroscience Institute Göttingen during my Erasmus stay. I would like to thank her for her support and criticism. I wish to acknowledge the scientific supervision provided by Nuno Raimundo Ph. D and King Faisal Yambire M. Sc., I am grateful for the support, sharing knowledge and experience with me. Assistance provided by Catia V. Diogo, Ph. D., Lorena Fernandez-Mosquera, Ph. D. and Christine Rostosky, M. Sc. was greatly appreciated. I wish to acknowledge all my co-workers of the friendly environment that they created for me. The goals of this internship were achieved by usage of facilities of the European Neuroscience Institute Göttingen and Institute of Cellular Biochemistry of University Medical Center Göttingen.

*List of content*

**List of figures**

# 1 Introduction

Putative interdependence between mechanisms of endocytosis and the maintenance of mitochondrial structure and function exists since several proteins are necessary for proper mitochondrial function. Particularly, ATPase EHD1, GTPases dynamin-2 and dynamin-related protein-1 (Drp1) are involved in mitochondrial fission [1]. Endophilin B1 is necessary to preserve mitochondrial morphology, and both endophilins B1 and B2 are essential for sequestration of the depolarized mitochondria and inner mitochondrial membrane (IMM) protein degradation [2] [3]. Moreover, inhibitors of clathrin mediated endocytosis also affect mitochondria: Endosidin9 and tyrosine kinase inhibitor tyrphostin A23 uncouple mitochondrial oxidative phosphorylation [4]. Massive endocytosis depends on mitochondrial permeability transition pore openings, subsequent coenzyme A (CoA) release, acyl CoA synthesis, and membrane protein palmitoylation [5]. The main goal of this work is to investigate the effects of defective endocytosis resulting from knock-out of synaptojanin-1 and endophilin-A on mitochondria. Firstly, it was tested whether aforementioned endocytic proteins alter mitochondrial function. Thereafter, pathways affected by the knock-out of these proteins were studied to determine causality regarding the observed phenotypes.

## 1.1 Mitochondria

Mitochondria are crucial organelles of the eukaryotic cell. They are responsible for the formation of heme and the biosynthesis of iron-sulfur clusters. (Stehling, 2014). Their roles are also energy production in the form of ATP and phospholipid and calcium buffering (Duchen, 2000). Moreover, they are necessary for activation of the intrinsic cell death pathway and capable of apoptosis induction (Green and Reed, 1998). Mitochondria have inner and outer membranes that are responsible for maintenance and isolation of two different aqueous compartments: the inter-membrane space and the matrix. The inner mitochondrial membrane encompasses the respiratory chain where oxidative phosphorylation takes place in order to produce ATP (Mitchell, 1961; Mitchell and Moyle, 1967). Mitochondria earned the title of ‘the powerhouse of the cell’ because they house the machinery for aerobic ATP generation (McBride et al., 2006). Precise mitochondrial function relies on accurate coordination between nuclear and mitochondrial encoded genes using diverse anterograde and retrograde signalling pathways (Ryan and Hoogenraad, 2007).

Thus, faulty mitochondrial function has a great impact on to cell, and consequently on the whole organism. Defective mitochondria are especially harmful in highly energetic, polarized cells like neurons (Park et al., 2001). Neurons are dependent on mitochondrial oxidative phosphorylation and their capability for glycolysis is restricted (Herrero-Mendez et al., 2009; Bolanos et al., 2010). Dysfunctional mitochondria have been linked to different diseases of the Central Nervous System, for example Alzheimer’s, Huntington’s and Parkinson’s diseases. Moreover, they are related to Leigh syndrome, Freidreich’s ataxia and motor neuron disease. (Santorelli et al., 1993; Mecocci et al., 1994; Panov et al., 2002; Valente et al., 2004) [6].

## 1.2 Endocytosis

Endocytosis is the process performed by cells not only to consume extracellular constituents, nutritional and regulatory proteins, but also to recycle membrane added during exocytosis. Substrate is surrounded by inward folding of the plasma membrane, which subsequently forms an intracellular vesicle. In addition, proteins and peptides are transported into the cell by receptor-mediated endocytosis: they are bound to specific cell surface receptors and quickly internalised by the cell (Grant and Donaldson, 2009). Next step is clustering of the proteins in the form of coated pits that invaginate to form

intracellular coated vesicles. Coated pits contain a specific set of transmembrane proteins, the coat is composed predominantly of a protein named clathrin [7]. Receptor mediated endocytosis is graphically represented in figure 1.1.

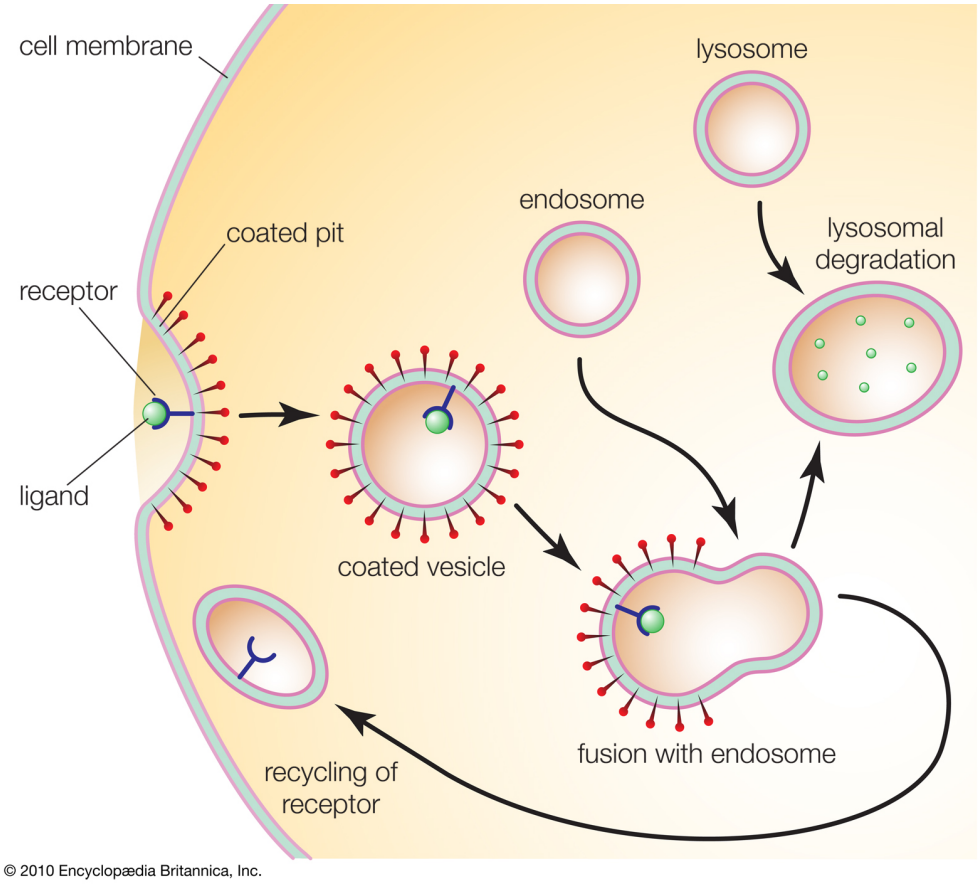


*Figure 1.1 Receptor mediated endocytosis. Image originally published in [8].*

In this project, the focus was on endophilin-A1, A2 and A3, a family of adaptor proteins that have a role in the endocytic process (Saheki and De Camilli P, 2012). The endophilins contain a Bin/Amphiphysin/Rvs (BAR) domain, which facilitates their binding to the neck of endocytic pits (Saheki and De Camilli P, 2012). Their SH3 domain is responsible for interaction with synaptojanin-1, a PI(4,5)$P_2$-phosphatase involved in the shedding of endocytic proteins when reaction is completed (Milosevic et al, Neuron 2011). Endocytic proteins are linked to various diseases such as Huntington's disease, Alzheimer's disease, Down syndrome, Parkinson's disease, unspecific tauopathies, cognitive deficits, seizures, and cancers [9] [10] [11] [12] [13] [14] [15] [16] [17] [18] [19] [20] [21] [22].

## 1.3 Summary

In the following chapter, the theoretical background on mitochondria and clathrin-mediated endocytosis is presented to provide the context in which the findings will be interpreted. The third section is a description of all methods applied in the research that mostly belong to molecular biology, biochemistry and microscopy. The subsequent chapter includes results of performed experiments which indicate presence of mitochondrial and lysosomal dysfunction and perturbed PI3K/AKT/mTOR signaling. They are discussed in another, fifth section. The conclusions can be found in the last section.

# 2 Theoretical background

## 2.1 Clathrin-mediated endocytosis

Endocytosis is necessary for the neurons to recycle membranes of synaptic vesicles (Saheki and De Camilli P, 2012). Dynamin, synaptojanin-1 and endophilin-A are functional partners in synaptic vesicle recycling participating in interrelated actions in clathrin-mediated endocytosis (CME) and actin dynamics in neurons (Schuske et al., 2003; Verstreken et al., 2003, Milosevic et al., 2011). Efficient endocytic and synaptic vesicle (SV) recycling mechanisms are necessary to maintain the high activity of the nervous system. Flawed endocytosis and SV recycling are related to neurodegeneration and neurodegenerative diseases, although, the molecular mechanisms should be elucidated (Esposito et al., 2012; Heutink and Verhage, 2012; Saheki and De Camilli, 2012; Schreij et al., 2016).

### *2.1.1 Synaptojanin-1*

The clathrin-coated vesicles (CCVs), during the transport to target sites, are uncoated by synchronized action of synaptojanin-1 (SYNJ1), the chaperone Hsc70 and its cochaperone auxilin. Hsc70 and auxilin are responsible for the clathrin disassembly (Ungewickell et al., 1995), whereas SYNJ1 dephosphorylates $PI(4,5)P_2$, by this means shedding the adaptor proteins (Cremona et al., 1999; Mani et al., 2007). Knock-out of the Synj1 gene in mice results in augmented $PI(4,5)P_2$ levels, flawed uncoating of clathrin, accumulation of CCVs, endocytic delays, and severe neurological phenotypes (weakness, ataxia), causing perinatal lethality (Cremona et al., 1999). Very similar phenotypes are observed in the auxilin and endophilin knock-out mice what demonstrates a close functional interaction between these proteins. (Milosevic et al., 2011; Yimet al., 2010) [23]. Interestingly, Synaptojanin-1 dysfunction might be relevant in Down Syndrome (DS) [14] [17]. The gene of SYNJ1 is located on chromosome 21 and present in triplicate in DS. Moreover, elevation of SYNJ1 can ameliorate synaptic and behavioural deficiencies in a mouse model of Alzheimer Disease [24].

### *2.1.2 Endophilin-A*

The three mammalian endophilin-A (A1-A3) function as hubs of a protein network that regulates cargo packing, bud constriction, actin assembly and recruitment of factors necessary for fission and uncoating (Saheki and De Camilli, 2012). All three proteins play key roles in clathrin-mediated endocytosis (Farsad et al., 2001; Ringstad et al., 1997, 1999, 2001; Verstreken et al., 2002; Milosevic et al., 2011) and clathrin-independent endocytosis (Boucrot et al., 2015). Putative model of clathrin-coated vesicle fission and uncoating at synapse is graphically represented in figure 2.1. Each endophilin contains the BAR-domain that senses and induces membrane curvature, and SH3-domain that recruits the GTP-ase dynamin and the $PI(4,5)P_2$ phosphatase synaptojanin-1 to clathrin-coated pits (Saheki and De Camilli, 2012). Upon fission, $PI(4,5)P_2$ degradation starts the shedding of clathrin adaptor proteins from the endocytosed membranes, conclusively resulting in the uncoating of SVs (Schuske et al, 2003; Verstreken et al., 2003; Milosevic et al., 2011), which is facilitated by auxilin and Hsc70 (Ungewickell, 1985; Chappell et al., 1986; Yim et al., 2010). Endophilins A1 and A3 are brain-enriched, whereas endophilin A2 is ubiquitous (Ringstad et al., 1997, 1999). Endophilin-A as endocytic adaptors have important role in membrane dynamics at the neuronal synapse (Ringstad et al., 1999; Verstreken et al., 2002; Milosevic et al., 2011; Saheki and De Camilli, 2012). Endophilin-A are also related to the ubiquitin-proteasome system via direct interaction with the Parkinson's disease (PD)-related E3-ubiquitin ligase parkin (Trempe et al., 2009). Furthermore, CBL/CIN85-endophilin complex downregulates receptor internalization (Soubeyran et al., 2002; Petrelli et al., 2002).

The total knock-out of endophilin-A causes perinatal lethality and impaired synaptic transmission. Fractional endophilin-A absence leads to severe neurological defects, including epilepsy and neurodegeneration. Remarkably, level of endophilin-A is increased in the brains of PD patients (Shi et al., 2009). Parkin is significantly augmented due to endophilin-A triple knock-out (Cao et al., 2014). Most likely, diminished endophilin availability impairs capacity to form autophagosomes, in consequence autophagy is reduced so ubiquitinated proteins accumulate in the cytoplasm and proteasome is saturated. Additional accumulation of unwanted proteins over time influences neuronal function, health and leads to neurodegeneration. Interestingly, pathway analysis of the transcriptional signatures of TKO hippocampi indicates that one of the most significantly enriched pathways is mitochondrial dysfunction [25].

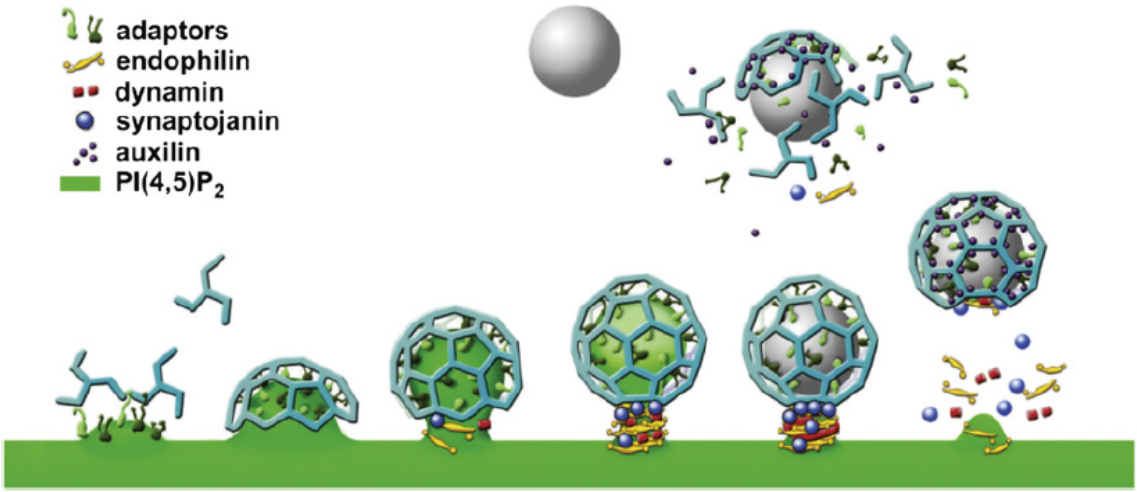


*Figure 2.1. Putative Model of Clathrin-Coated Vesicle Fission and Uncoating at Synapse. Image originally published in [23].*

### *2.1.3 Putative links between mitochondrial function and endocytosis*

Endophilin B1 (EB1), also known as Bif-1 or SH3GLB1, belongs to the endophilin protein family and was firstly recognized as a Bax-binding protein. Bax is a pro-apoptotic member of the Bcl-2 protein family responsible for release of apoptogenic factors from the mitochondria in order to commence the caspase cascade. Moreover, EB1 probably has a role in mitochondrial fission and COPI-vesicle formation. EB1 also interacts with Beclin1 through ultraviolet irradiation resistant-associated gene (UVRAG) to control the activation of the class III PI3 kinase, PI3KC3 and the induction of autophagy in mammalian cells. Furthermore, endophilin B1 plays a role in the early stages of autophagosome formation and maybe in the biogenesis and/or expansion of phagophores [2].

EB1 is necessary to preserve mitochondrial morphology. The fraction of EB1 located in mitochondria probably contributes to the conservation of the mitochondrial membrane structure. Another member of endophilin family, endophilin B2 (EB2) is related to cytoskeletal architecture and possibly to Down syndrome. Both endophilins B are equally vital for sequestration of the depolarized mitochondria and IMM protein degradation. EB1 and EB2 form heterodimers that aggregate into foci, translocate to mitochondrial fragment, and promote IMM degradation [3].

Recently, dynamin-2 and dynamin-related protein-1 (Drp1) were reported as GTPases involved in mitochondrial fission. Moreover, ATPase and endocytic protein, EHD1, was implied as another regulator of mitochondrial fission working under a novel premise of endocytic protein regulation of

mitochondrial homeostasis. Depletion of both, dynamin-2 and Drp1 or EHD1 results in a static and elongated network of mitochondria in the cell; however, EHD1- depleted cells stay responsive to staurosporine, while Dynamin-2 and Drp1- depleted cells are insensitive to this drug. Furthermore, the VPS35 retromer subunit and the retromer complex were indicated to be involved in PD and mitochondrial fission, demonstrating a previously unknown link between an endocytic regulatory complex and a non-endocytic organelle (Follett et al., 2014; Kumar et al., 2012; Sharma et al., 2012; Struhal et al., 2014; Tang et al., 2015; Vilarino-Guell et al., 2011; Zimprich et al., 2011) [1].

Mitochondrial uncouplers not only dissipate an electrochemical proton gradient across the inner mitochondrial membrane, that is necessary for ATP production, but also disrupt several cellular processes such as vesicular trafficking, principally through energy depletion. Some inhibitors of CME, namely Endosidin9 (ES9) and tyrosine kinase inhibitor tyrphostin A23 (TyrA23), uncouple mitochondrial oxidative phosphorylation. Their impact on CME does not result from mitochondrial dysfunction and ATP depletion, instead, it depends on their uncoupling activity at other membranes, causing acidification of the cytoplasm. Acidification leads to a huge rise in the lifetimes of clathrin and associated adaptors and a decrease of the phosphatidylinositol 4,5-biphosphate ($PI(4,5)P_2$), thus, it probably inhibits clathrin-coated pits formation [4].

Furthermore, massive endocytosis (MEND) relies upon mitochondrial permeability transition pore (PTP) openings, subsequent coenzyme A (CoA) release, acyl CoA synthesis, and membrane protein palmitoylation. The MEND pathway might be partially responsible for constitutive and pathological plasmalemma turnover depending on mitochondrial stress signalling. Interestingly, mitochondria respond to immense calcium transients what triggers MEND in BHK cells. It was demonstrated that CoA and acyl CoAs are intermediates in the pathway and oxidative stress promotes acyl CoA-dependent endocytosis without PTP openings [5].

## 2.2 Mitochondria

Mitochondria are organelles dynamically adjusting to environment by fission and fusion. Their life cycle full of extensive post-translational modifications start with biogenesis and ends with mitophagy; mitochondrial life cycle is graphically represented in figure 2.2. Mitochondria have a key role in metabolism of glucose, fatty acids, and amino acids. They are responsible for production of ATP affecting redox environment, oxidative stress, pH, and other metabolites like acetyl-CoA and NAD+ that influence many aspects of cellular metabolism. Environmental stresses can be addressed thanks to the multifaceted interaction of mitochondria, cytosolic factors and, ultimately, the nucleus.

### *2.2.1 Mitochondrial dynamics*

The following processes regulate mitochondrial morphology:

i. Mitochondrial fission results in more numerous mitochondria and, when excessive, smaller and more circular mitochondria. If fission is caused by pathologic stress, mitochondria with low membrane potential are marked for mitophagy by accumulation of Pink1 and recruitment of Parkin.
ii. Mitochondrial fusion generates fewer, larger and more elongated mitochondria. Mitochondrial fusion is coordinated by mitofusins on the outer mitochondrial membrane (OMM) and OPA1 on the inner mitochondrial membrane (IMM).
iii. Mitophagy is the selective autophagy of damaged mitochondria and a key factor of proper mitochondrial quality control.

iv. Mitochondrial biogenesis: the process that increases mitochondrial number and/or content through increased expression of both mitochondrial and nuclear transcripts, which is regulated by PGC-1 alpha, PGC-1 beta, and the PGC-related coactivator PRC. PGC-1 alpha works in tandem with nuclear respiratory factor 1 (NRF-1) to trigger the expression of nuclear-encoded mitochondrial genes. Overexpression of PGC-1 alpha is sufficient to drive mitochondrial biogenesis.

PINK1 and Parkin not only regulate mitophagy, they are also involved in leading the localized translation of nuclear-encoded respiratory chain complex mRNAs on the OMM. This indicates that there is a link between mitochondrial quality control and oxidative phosphorylation (OXPHOS) [26].

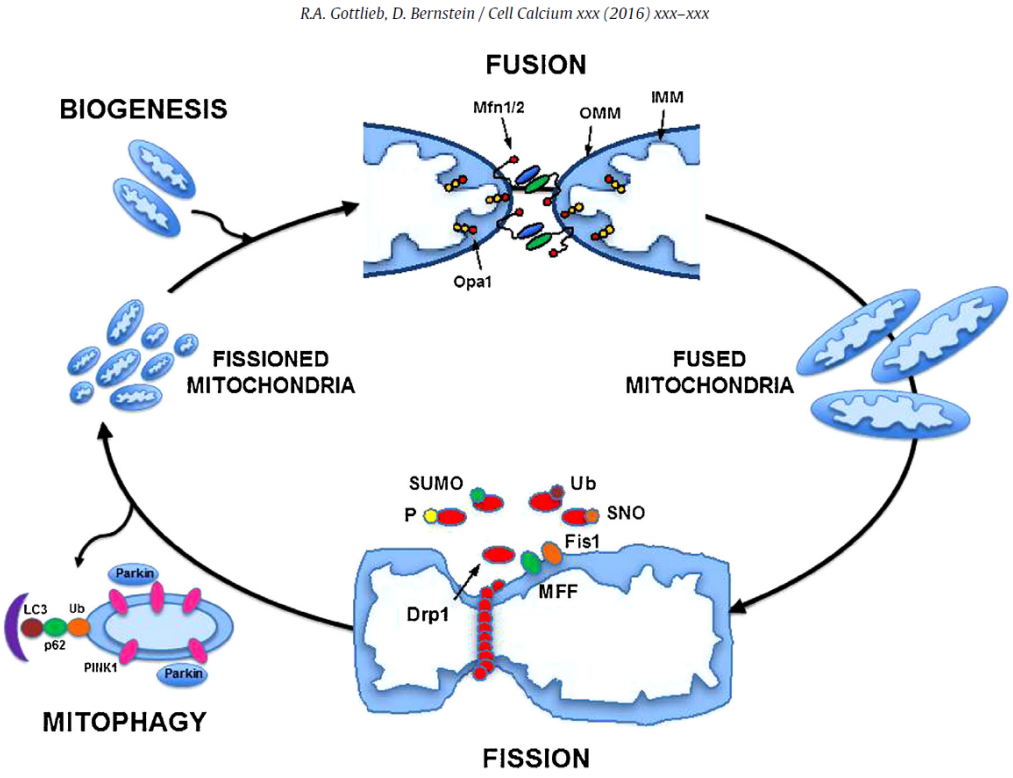


*Figure 2.2. Mitochondrial dynamics. Image originally published in [26].*

### *2.2.2 PGC-1α regulation*

Expression of gene PGC-1α rises in situations of energy stress, for example exercise, fasting, or cold exposure. There is a redundancy in the signalling pathways controlling PGC-1α on both, transcriptional and posttranslational level, and some of them interact functionally and affect the abilities of others. PGC-1α is controlled by following signalling pathways: AMPK, PKA, AKT, SIRT1 and p38 MAPK and posttranslational alterations influence various areas of the protein, what enables rapid, complex, and flexible regulation of PGC-1 α activity [27].

### *2.2.3 Respiration*

The mitochondrial respiratory chain is built of five protein complexes: NADH-ubiquinone oxidoreductase as Complex I, succinate-ubiquinone oxidoreductase as Complex II, ubiquinone cytochrome-C oxidoreductase as Complex III, cytochrome C oxidase as Complex IV, and ATP synthase

as Complex V. Electron transfer starts in Complex I which receives electrons from NADH. These electrons are transported to Complex III via ubiquinone and then to Complex IV via cytochrome C. Transfer of electrons is accompanied by the proton transfer responsible for generating a gradient which provides the energy needed for ATP synthesis (Mitchell and Moyle, 1968) [28].

### *2.2.4 Reactive Oxygen Species*

Reactive oxygen species (ROS), mostly superoxide, are by-products of the respiratory chain, which are created in the mitochondria at Complex I and Complex III. Normally, mitochondrial antioxidant defences, such as superoxide dismutase, convert the superoxide to hydrogen peroxide and then to water. In pathological conditions superoxide level may increase above the defence capacity due to increased production or antioxidant defence attenuation [29].

### *2.2.5 Glycolysis*

Glycolysis is the metabolic pathway responsible for conversion of glucose into pyruvate in cytoplasm, which produces adenosine triphosphate (ATP). The whole pathway of glycolysis consists of 10 steps of chemical reactions and each of them is catalysed by a specific enzyme. Figure 2.3 presents these 10 steps and 10 specific enzymes, respectively hexokinase (HK), phosphoglucose isomerase (PGI), phosphofructokinase (PFK), aldolase, triosephosphate isomerase (TPI), glyceraldehyde 3 phosphate dehydrogenase (GAPDH), phosphoglycerate kinase (PGK), phosphoglycerate mutase (PGM), enolase, and pyruvate kinase (PK).

Multiple metabolic pathways depend on glycolysis as a source of metabolites, such as glucose being a breakdown product of glycogen or starch and taking part in gluconeogenesis; fatty acids can be produced using acetyl coenzyme A (acetyl-CoA) from the pyruvate, which is supplied by glycolysis; also the amino acid, alanine, is synthesized through the pyruvate. Moreover, glucose and glucose-6-phosphate are intermediates in the conversion of other sugars and they are involved in nucleotide synthesis. In the tricarboxylic acid cycle (TCA) pyruvate is converted into acetyl-CoA and carbon dioxide ($CO_2$) within the mitochondria. The acetyl-CoA then enters the TCA cycle where it is entirely oxidized to $CO_2$ and water ($H_2O$), what generates more energy than glycolysis [30].

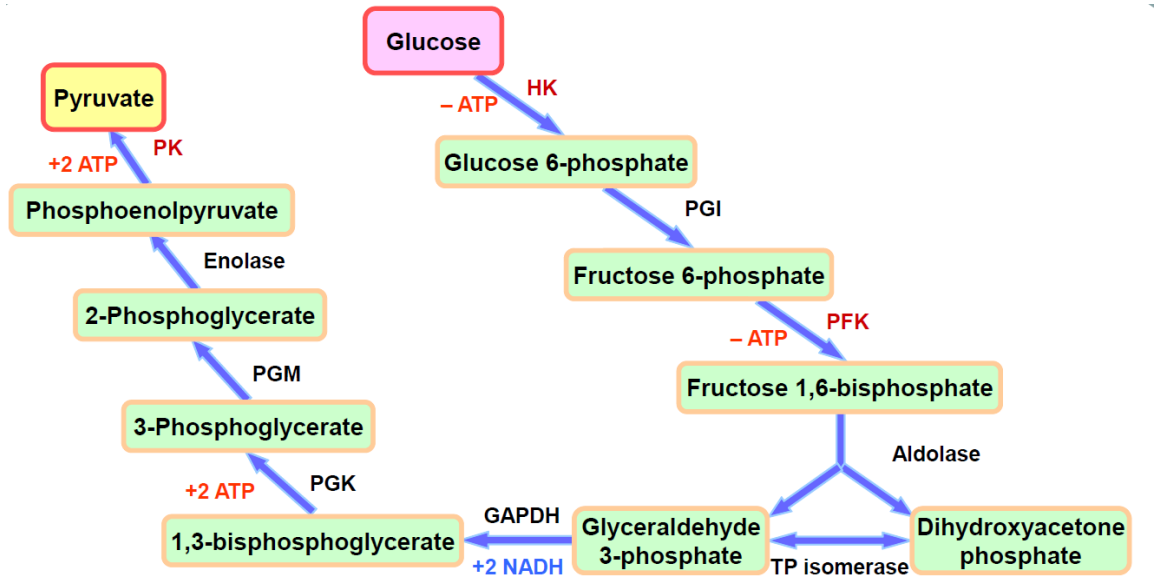


*Figure 2.3 Schematic diagram of glycolysis. Image originally published in [30].*

### *2.2.6 Protein import*

Impaired mechanism responsible for the targeting, import, and precise assembly results in improper mitochondrial function and shape because most of mitochondrial proteins are encoded in the nucleus. After transcription from the nuclear genome, mRNAs are translated in the cytosol to precursor proteins which have signals for targeting to specific mitochondrial compartments. Then, these proteins are attended by molecular chaperones, unfolded, and imported into mitochondria by the translocase of the outer membrane complex (TOM). Next, specific precursors are directed through the import machinery of the inner membrane complex (TIM) into the mitochondrial matrix dependently of membrane potential. In the end, these precursors are cleaved of their import sequences and are refolded by intramitochondrial proteins [31].

## 2.3 Cross talk between mitochondria and lysosomes

Mitochondria are regularly interacting with the rest of the cell; in consequence, mitochondrial defects affect other organelles, including their function and biogenesis. Genetic abnormalities in genes encoding mitochondrial proteins cause disorders called "mitochondrial diseases", in which lysosomes and peroxisomes are also reported to be altered structurally and functionally. Additionally, secondary mitochondrial defects are present in many peroxisomal and lysosomal diseases.

Lysosomes are not only the endpoint of the endocytic and autophagic pathways but also they are involved in other cellular processes like amino acid sensing, exocytosis, plasma membrane repair, transcriptional regulation. Furthermore, they function as a reservoir of amino acids, metabolites, and ions. Due to the fact that lysosomes are linked to numerous metabolic functions, a coordination with other organelles related to metabolism is necessary. Complexity of cross-talk between mitochondria and lysosomes results, in part, from the role of lysosomes at the end of the mitochondrial life cycle: damaged mitochondria are degraded via autophagy.

In general, available literature demonstrates that acute mitochondrial malfunction triggers TFEB signalling and promotes lysosomal biogenesis in proliferating cells. Interestingly, distinct mechanisms are activated because of chronic mitochondrial stress and in post-mitotic tissues: acute mitochondrial stress triggers lysosomal biogenesis, in an AMPK- and TFEB/MITF-dependent manner, while chronic mitochondrial stress, on contrary, represses lysosomal biogenesis. Moreover, chronic mitochondrial stress leads to lysosomal malfunction [32] [33] [34].

Lysosomal storage diseases (LSDs) result from mutations in genes encoding lysosomal proteins and are characterized by the storage of diverse molecules inside the lysosomes preventing them from functioning correctly. Data published recently indicate that not only lysosomes but also other cellular organelles are affected, thus, a possible crosstalk between organelles may be recognized as an element of LSD pathogenesis. It is known so far that defective lysosomes lead to mitochondrial dysfunction. Interestingly, excess of impaired mitochondria resulting from insufficient autophagy is not enough to explain observed characteristics. Ultrastructural abnormalities in mitochondrial morphology, decline of mitochondrial membrane potential and flawed mitochondrial $Ca^{2+}$ homeostasis have been detected in a few lysosomal diseases [35] [36].

## 2.4 PI3K/AKT/mTOR pathway

The mechanistic target of rapamycin (mTOR) regulates eukaryotic cell growth and metabolism using sensory information about environmental inputs, for example nutrients and growth factors. mTOR has a crucial role in coordination of many important cell processes, from protein synthesis to autophagy. Roles of mTOR are summarized in the figure 2.4. Furthermore, perturbed mTOR signalling is related

to the progression of cancer and diabetes, also to the aging process. mTOR is a serine/threonine protein kinase in the PI3K-related kinase (PIKK) family that forms the catalytic subunit of two protein complexes named mTOR Complex 1 (mTORC1) and Complex 2 (mTORC2).

### *2.4.1 mTOR Complex 1*

It is necessary for cells not only to boost production of proteins, lipids, and nucleotides but also to inhibit catabolic pathways like autophagy in order to grow and divide. mTORC1 is responsible for controlling all of these processes, thus, adjusts the balance between anabolism and catabolism responding to environmental cues. mTORC1 stimulates protein synthesis mostly through the phosphorylation of the two essential effectors: p70S6 Kinase 1 (S6K1) and eIF4E Binding Protein (4EBP). S6K1 is directly phosphorylated by mTORC1 on its hydrophobic motif site (Thr389) and, later, phosphorylated and activated by PDK1 in order to, subsequently, phosphorylate and activate a few substrates that foster mRNA translation initiation.

mTORC1 is triggered by feeding to stimulate growth and energy storage in tissues like the liver and muscle; on the other hand, under nutrient deprivation, it is suppressed to conserve limited resources. mTORC1 stimulates lipid synthesis through the sterol responsive element binding protein (SREBP) and the synthesis of nucleotides necessary for DNA replication and ribosome biogenesis in growing and proliferating cells. Moreover, mTORC1 promotes a switch in glucose metabolism from oxidative phosphorylation to glycolysis. mTORC1 boosts the translation of the transcription factor HIF1α which is responsible for the expression of some glycolytic enzymes.

Additionally, feeding also results in higher serum amino acid levels because of the absorption of dietary proteins. mTORC1 activity is deeply connected to diet-induced variations in amino acid concentrations due to the fact that amino acids are sources of energy and carbon for numerous metabolic pathways besides being key building blocks of proteins. Furthermore, mTORC1 acts in answer to intracellular and environmental cues such as low ATP levels, hypoxia or DNA damage that are conflicting with growth. Stress responsive metabolic regulator AMPK is activated due to a decrease in cellular energy charge and, subsequently, inhibits mTORC1 directly, through the phosphorylation of Raptor and indirectly, through phosphorylation and activation of TSC2 (Gwinn et al., 2008; Inoki et al., 2003b; Shaw et al., 2004). It is also known that mTORC1 senses glucose through more than one mechanism: lack of glucose leads to inhibition of mTORC1 even in cells missing AMPK, through inhibition of the Rag GTPases (Efeyan et al., 2013; Kalender et al., 2010). Moreover, mTORC1 is inhibited due to hypoxia not only through AMPK activation, but also through the induction of REDD1.

### *2.4.2 mTOR Complex 2*

In contrast to mTORC1 that controls cell growth and metabolism, mTORC2 regulates proliferation and survival mostly by phosphorylating various members of the AGC family of protein kinases. One of the crucial roles of mTORC2 is the phosphorylation and activation of the serine/threonine kinase AKT, which is most important effector of insulin/ PI3K signalling. The subunit mSin1 of mTORC2 consists of a phosphoinositide- binding PH domain that is common among PI3K regulated proteins and necessary for the insulin-dependent control over mTORC2 activity. The mSin1 PH domain is responsible for suppression of mTORC2 catalytic activity while insulin is not present, while binding to PI3K-generated PIP3 at the plasma membrane diminishes this autoinhibition (Liu et al., 2015). Moreover, data published so far indicate that there is a positive-feedback loop: mSin1 is also phosphorylated by AKT, whereas partial activation of AKT boosts the activation of mTORC2. Interestingly, a negative feedback loop between mTORC1 and insulin/PI3K signalling was demonstrated, thus, mTORC2 signalling is also under control of mTORC1. Furthermore, S6K1 inhibits mTORC2 activation through

the phosphorylation-dependent degradation of insulin receptor substrate 1 (IRS1) (Harrington et al., 2004; Shah et al., 2004). Notably, mTORC1 having control of PI3K and mTORC2 signalling is significant for the pharmacological targeting of mTOR in disease [37].

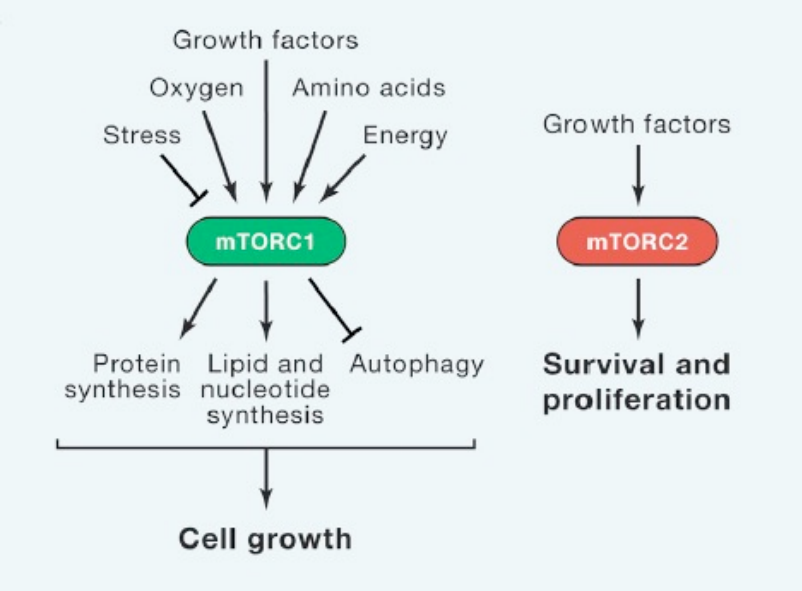


*Figure 2.4. Roles of mTOR. Image originally published in [37].*

### *2.4.3 Physiological Roles of mTOR*

Changes in whole-body metabolism have to address any fluctuations in amount of accessible energy sources resulting from fasting or feeding to sustain homeostasis. Quantities of nutrients and growth factors decrease due to starvation, what leads to a catabolic state in which energy stored before is used to provide for fundamental functions. On the other hand, a shift toward anabolic growth and energy storage is required in presence of elevated amount of nutrients in the fed-state. Available literature demonstrates that mTOR signalling is not only essential for coordination of anabolism and catabolism at the cellular level but also for proper control over metabolism at the organismal level.

It is important to mention that constitutive mTOR activation results in undesirable physiological outcomes, showing that the accurate adjustment of mTOR signalling to answer environmental cues is essential. Furthermore, mTOR is crucial for regulation of multiple neurological processes, such as neural development, circuit formation and the neural control of feeding (reviewed in Lipton and Sahin, 2014). It was confirmed that both, mTORC1 and mTORC2 signalling is critical for correct brain development by showing that the deletion of Raptor or Rictor in neurons results in decreased neuron size and premature death.

Moreover, human patients with Tuberous sclerosis complex (TSC), which is characterized by hyperactive mTORC1 signalling, suffer from a variety of neurological disorders, among others epilepsy, autism, and benign brain tumors. It is worth mentioning that impaired autophagy is tightly related to the pathogenesis of neurodegenerative disorders, such as Parkinson's disease and Alzheimer's disease (AD), while mTORC1 regulates autophagy. It was shown that suppression of mTOR signalling is advantageous on mouse models of AD [37].

### *2.4.4 mTOR regulates iron metabolism*

Due to the fact that body's levels of iron have to be kept within strict limits for cells to function properly, both, excess or shortage of iron may significantly affect health of an individual. Iron is a crucial cofactor in various biological processes, for example oxygen transport, cellular respiration and DNA synthesis. Ferrous iron reacts with hydrogen peroxides or lipid peroxides to produce hydroxyl or lipid radicals; thus, overabundance of iron is highly toxic. On the other hand, deficit of iron leads to cellular growth arrest and death.

The iron level in the body is under the meticulous control of at least two mechanisms: iron regulatory proteins (IRPs) and RNA stem-loop iron regulatory elements (IREs) mechanism and the transcriptional regulation of hepcidin. IRPs are responsible for maintenance of cellular iron homeostasis, as they regulate specific mRNAs encoding proteins of iron uptake, export, storage and utilization. The IRPs bind to IREs which are localized in untranslated regions (UTRs) of diverse mRNAs whose products are involved in iron metabolism, such as transferrin receptor 1 (TfR1), ferritin heavy (FTH1) and light chain. IRE/IRP complex that was formed within the 5'UTR of e. g. FTH1 mRNA prevents its translation, on the other hand IRP binds to IREs in the 3'UTR of e. g. TfR1 mRNA to restrain its degradation. Moreover, Hepcidin inhibits intake of iron from the gastrointestinal tract and discharge of iron for macrophages by binding to the iron-transport protein ferroportin, leading in consequence to its destruction.

Iron as a cofactor and its reliable distribution are necessary for multiple functions of mTOR. Literature so far indicates that mTOR pathway regulates iron metabolism and homeostasis employing at least two mechanisms: phosphorylation to preserve Iron-Sulfur Cluster Assembly Enzyme (ISCU protein) and inhibition of Tandem zinc finger (TZF) protein tristetraprolin (TTP) expression independently. ISCU is an mTOR kinase target, and mTORC1-mediated stabilization of ISCU protein is possible thanks to phosphorylation of S14. Moreover, mTORC1 has impact on ISCU gene expression and function, and hence boosts ISC assembly. Silencing of ISCU leads to disruption of ISC biogenesis, inadequate activation of the IRP1 and turmoil in intracellular iron homeostasis. Additionally, labile ISC is necessary for IRP1 to register cytosolic iron and oxidative stress. Decreased activity of mTORC1 results in deficiency of ISCU and, in consequence, enhancement of the binding activity between IRP and IRE.

mTOR activity prevents the transcription and destabilization of Tristetraprolin (TTP) mRNA, while TTP attunes TfR1 stability and changes cellular iron flux through destabilization of mRNAs of dispensable iron-containing proteins and release of iron to be consumed in essential processes. TTP induced by rapamycin negatively regulates the expression of TfR1, what results in decreased iron import and net iron loss from the cell. Notably, TTP also optimizes iron usage in iron deficiency by inhibition of the expression of ARE-containing iron-requiring proteins. Low levels of iron activate IRP1/2 in order to avoid greater iron deficit [38]. Role of mTOR in iron metabolism is graphically represented in the figure 2.5.

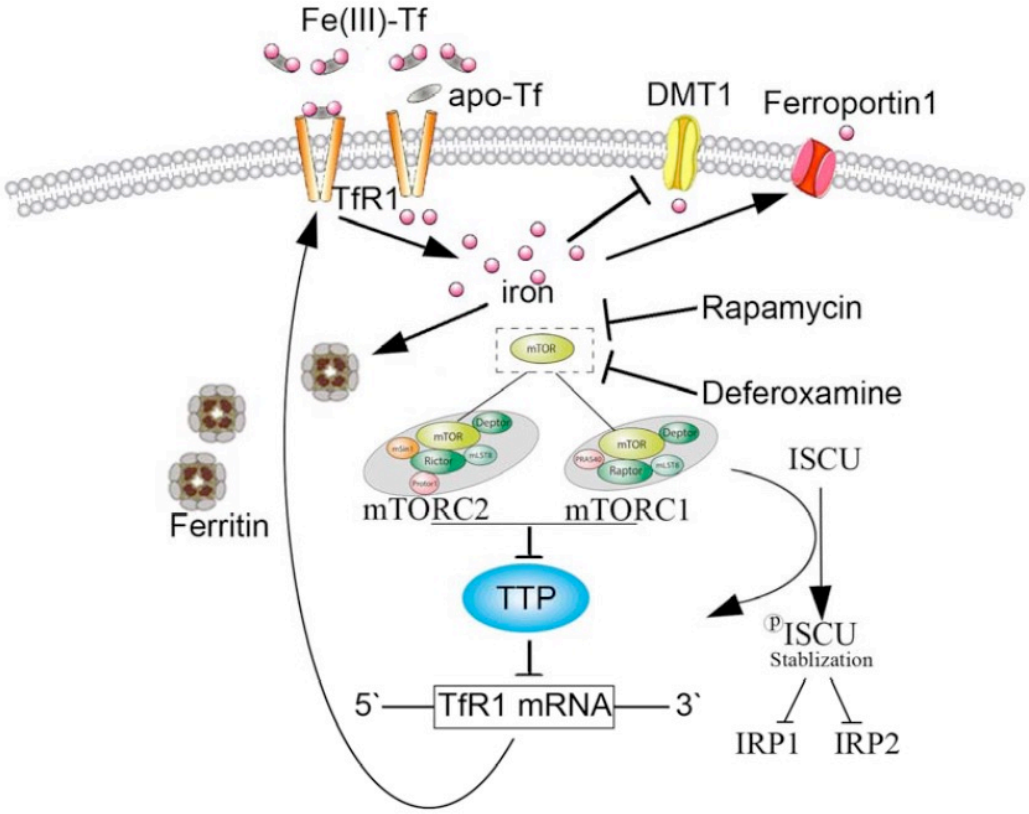


*Figure 2.5. mTOR regulates iron metabolism. Image originally published in [38].*

## 2.5 Research objectives

Firstly, the Next-Generation Sequencing (NGS) raw data (RNA sequences) obtained from endophilin-A and synaptojanin-1 knock-out (KO) hippocampus and cortex were concatenated and mapped to the human genome. Then it was necessary to determine the expression levels of each transcript, and by comparing different sample groups establish a list of differentially regulated genes (DRGs), which were then validated by quantitative polymerase chain reaction (qPCR) using brains of newborn mice. Specifically, the expression of several genes, in particular genes related to mitochondria, which as a group were found significantly enriched in the DRGs, were then verified using qPCR and RNA isolated from mouse brains, performed as indicated in Murdoch, Rostosky *et al* (2016) [23]. These experiments aimed to confirm the reproducibility of the data, and explore the impact of endocytic defects on the expression of mitochondria-related genes.

The next step was determination of the amount of mitochondrial respiratory chain subunits (e.g., NDUFB8, SDHB, COX1, etc.), mitochondrial protein translocator subunits (e.g., Tomm20) and of markers of mitochondrial mass (e.g., VDAC, citrate synthase), and regulators of mitochondrial biogenesis (e.g. NRF1, GABPA, PGC1a) at protein level by *western* blotting. These experiments were performed in order to clarify whether the lower transcript levels of mitochondria-related genes may underlie a decrease in mitochondrial mass and how the levels of mitochondrial biogenesis regulators relate to the decrease in mitochondrial biogenesis. It was observed that the protein levels of mitochondrial proteins are mostly unchanged and do not follow any common trend, suggesting unaltered mitochondrial mass. Given that the transcriptional program of mitochondrial biogenesis is repressed,

the unaffected mitochondrial mass is likely a consequence of a decrease in the degradation of mitochondria. This process is dependent on autophagy, which is impaired in the endophilin mutants [25].

Afterwards, mouse embryonic fibroblasts (MEF) were prepared from synaptojanin-1 (SYNJ1 KO), endophilin-A triple knock-out (EndoA123 TKO) mice and respective littermate controls in order to determine whether the expression of mitochondria-related genes and mitochondrial mass are affected similarly as observed in the brain. MEF are a more amenable experimental system to test mechanistic connections, and thus it was verified if the effect of endocytic defects on mitochondrial biogenesis was also observed in MEF. For most experimental parameters that was the case here, and therefore the MEF can be used as a proxy experimental system. For the readouts in which the MEF do not phenocopy the brain, an alternative system would be primary neurons from synaptojanin-1 (SYNJ1 KO), endophilin-A triple knock-out (EndoA123 TKO) and corresponding littermate control mice.

Thereafter, mitochondrial function was evaluated by measurements of mitochondrial respiratory chain activity using live cells (MEF) by real-time respirometry. The experiment was performed with MEF growing in normal growth medium as well as in respiration-compulsive growth medium. Superoxide is a by-product of the respiratory chain and its production is increased in dysfunctional mitochondria. Proper mitochondrial membrane potential is necessary for efficient import and respiration and it is usually decreased in dysfunctional mitochondria. Flow cytometry was applied to assess superoxide levels using the MitoSox dye and mitochondrial membrane potential using JC1 dye.

Furthermore, since lysosomes are closely linked to the endocytic pathway, and the crosstalk between lysosomes and mitochondria can impact the function of both organelles, lysosomal mass was also measured, using LysoTracker Green dye and flow cytometry, while lysosomal proteolytic activity was recorded over time using DQ BSA dye and plate reader. Results of these experiments enable evaluation of lysosomal function which may affect mitochondrial capacity. To recognize functional iron deficiency gene expression and level of proteins related to iron metabolism were examined; amount of protein was assessed by *western* blotting. Activity of PI3K/AKT/mTOR pathway was evaluated based on ratio of amount phosphorylated protein to total amount of given protein detected by *western* blotting; following proteins were taken into consideration: total p70S6 Kinase 1 and phosphorylated by mTORC1 at Thr389, total AKT and phosphorylated by mTORC2 at S473.

Most of the data presented in the chapter number 4 *Results* were acquired and analyzed by the author on her own after adequate training since one of the side goals of this research was to maximize her independence in the laboratory and contribution to the project. There are few tasks that could not be performed by the author alone as they require specific qualifications: raw NGS data analysis, animal tissue extraction, MEF preparation, Seahorse and flow cytometer operation.

# 3 Methods

## 3.1 Animal models

Knock-out mouse models were previously generated [24] [39] using FLP-FRT system, in which the site-specific modifications are introduced into the genome of embryonic stem cells (ESCs) by homologous recombination. A targeting vector, which is DNA construct, is typically composed of a 5' homology arm, a positive selectable gene marker, here neomycin resistance gene (neo), and a 3' homology arm. The transfected targeting vector is integrated by homologous recombination as defined by the 5' and 3' homology arms. The endophilin A1 (SH3GL2) gene was inactivated in 129Sv/J ES cells by deleting the 3' end of the first coding exon, while the endophilin A2 (SH3GL1) gene was knocked-out by removing all coding exons following exon 1. The endophilin A3 (SH3GL3) conditional KO targeting vector was made by flanking a 1.8kb region including exon 1 with loxP sites and introducing an FRT site flanked neomycin cassette into intron 1. The targeting vector was electroporated into hybrid C57BL/6J-129S1/Sv mouse embryonic stem cells, which were then selected and screened by *southern* blotting.

Successfully transfected cells are positively selected by culturing ESCs in medium with neomycin. When the positive selection marker gene is flanked by loxP or FRT sites, it can be eliminated from targeted loci in ESCs or transgenic mice by expressing Cre recombinase (Cre) or flippase (FLP) in the recombinant ESCs through transfection with Cre- or FLP-expressing vector or by crossing the chimeric mice with Cre- or FLP-expressing transgenic mice. In this case chimeric animals were crossed with a FLP recombinase deleter strain to remove the neomycin selection cassette (Rodriguez et al., 2000). Successful deletion of the neomycin selection cassette in the FLP-positive off-spring was confirmed by PCR. Conditional mutants were then mated with a β-actin-Cre mouse (FVB/N-Tg(ACTB-cre)2Mrt/J; (Lewandoski and Martin, 1997) to disrupt the endophilin 3 gene ubiquitously, thus, a constitutive endophilin 3 knock-out could be generated. Targeting strategy is graphically represented in figure 3.1.

Similarly, inactivation of the synaptojanin-1 gene in ESCs from 129SV/J mice was accomplished by targeted disruption of its first coding exon. First of all, 103 bp from the 39 portion of this exon and 1571 bp of the adjacent intron were substituted by the neomycin cassette. In order to attain germline transmission of the mutant allele chimeric male mice were mated with C57BL/6 females. Accurate gene targeting in ESCs and transmission of the mutant allele to the offspring were tested by *Southern* blot analysis. *Western* blotting of brain tissue from homozygous mutant mice confirmed that neither synaptojanin 1 nor even fragments of the protein were expressed [40].

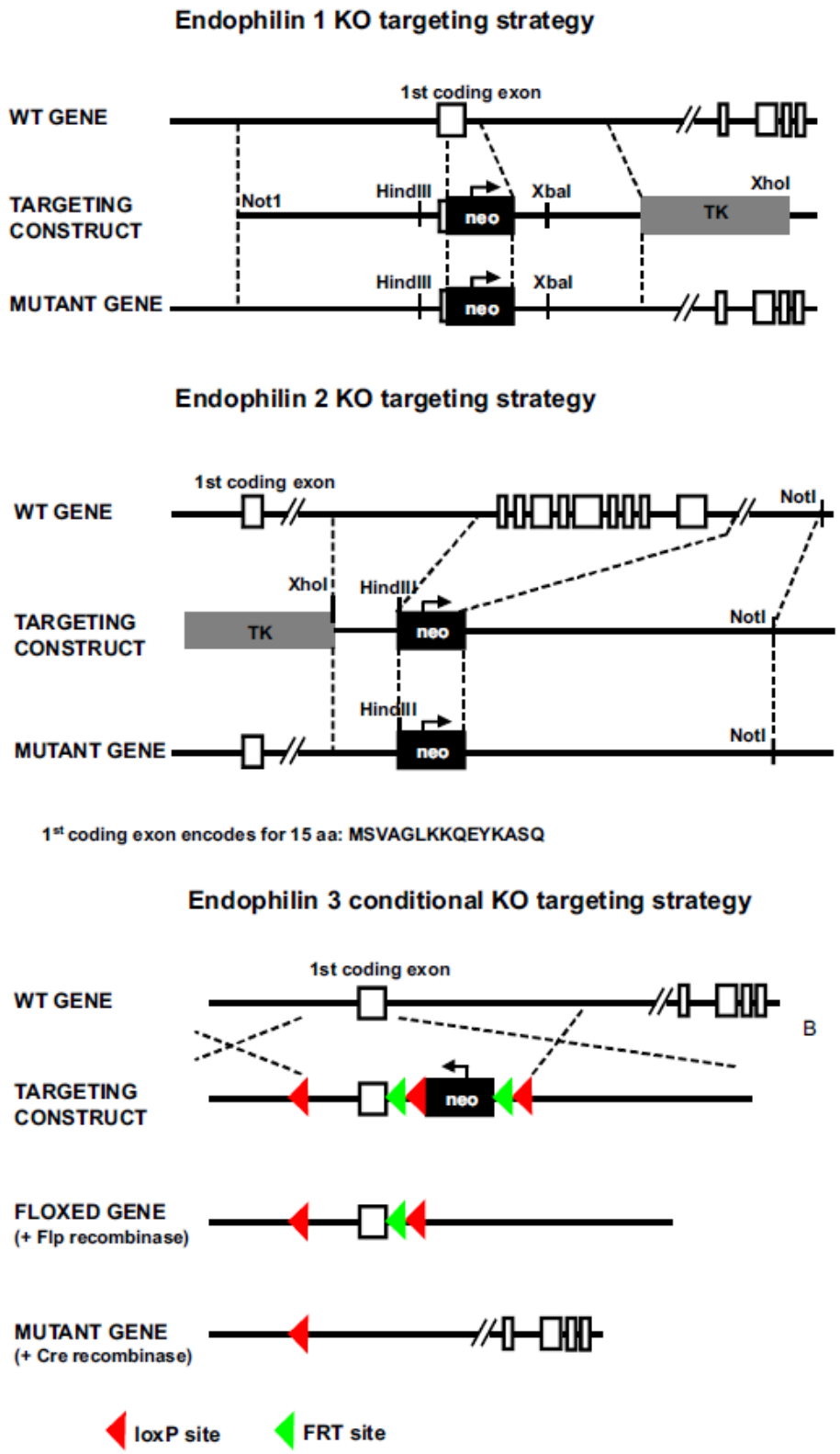


*Figure 3.1. Knock-out of endophilin-A using FLP-FRT system. Image originally published in* [24].

## 3.2 Cell work

### *3.2.1 Growth conditions*

Mouse embryonic fibroblasts (MEF) were grown in Dulbecco's Modified Eagle Medium high glucose medium (DMEM) supplemented with 10% fetal bovine serum (FBS) and 1% Penicillin/Streptomycin (P/S) at 37°C and 5% $CO_2$. All media and solutions used for cell work were either autoclaved or filtered.

## 3.3 Molecular biology

### *3.3.1 RNA isolation from cells*

Ribonucleic acid (RNA) isolation was done using CRYSTAL RNA Mini Kit BIOLAB. Cell pellets were in 2 ml Eppendorf tubes, where 400 µl of Lysis Solution RL and 4 µl of 2-Mercaptoethanol (β-SH) were added. After incubation at room temperature (RT) for 2 minutes, the pellet was re-suspended with a pipette. The samples were incubated at room temperature for 3 minutes and later were transferred at Spin Filter D placed in Receiver Tubes (2 ml) and centrifuged for 2 minutes at 10,000 x g. The column was discarded and 400 µl of 70% ethanol were added to the flow-through and mixed gently by pipetting. The flow-through with ethanol was transferred to Spin Filter R in Receiver Tubes and centrifuged for 2 minutes at 10,000 x g. After the column was placed and the flow-through discarded, 500 µl of Washing Solution HS were added to the Spin Filter R and the tubes were centrifuged for 1 minute at 10,000 x g. The column was shifted to a new collection tube and 700 µl of Washing Solution LS were added to the Spin Filter R. After Centrifugation at 10,000 x g for 1 minute, the flow-through was discarded and the Spin Filter R was placed in a new collection tube and it was centrifuged for 2 minutes at 10,000 x g to dry the membrane. The Spin Filter R was moved in a new 1.5 ml collection tube and 20 µl of RNAase-free water was added directly to the spin column membrane to elute the RNA. The tube was incubated for 1 minute at room temperature and was later centrifuged for 1 minute at 6,000 x g to collect the RNA.

RNA quantification and quality control was done using the Nanodrop. Only samples with concentration over 10 ng/µl were used for cDNA synthesis. RNA was stored at -80°C until it was used for cDNA synthesis.

### *3.3.2 RNA isolation from brains*

RNA was extracted from brain tissue using Trizol Reagent. 1 ml of Trizol Reagent was added to 50-100 mg of tissue and the homogenized sample was incubated for 5 minutes at room temperature. Afterwards, 0.2 ml chloroform per 1 ml of Trizol Reagent was added, the tubes were capped securely and shaken vigorously by hand for 15 seconds. Incubation for 2-3 minutes at room temperature was followed by centrifugation of the samples at 12,000 x g for 15 minutes at 4ºC. Then, the aqueous phase (about 0.5 ml) was removed by angling the tube at 45º and pipetting the solution out. The aqueous phase was poured into a new tube and 0.5 ml of 100% Isopropanol was added per 1 ml of Trizol Reagent used for the homogenization to the aqueous phase. Subsequently, samples were incubated at room temperature for 10 minutes and centrifuged at 12,000 x g for 10 minutes at 4ºC. The supernatant was removed from the tube, leaving only the RNA pellet which was washed with 1 ml of 75% Ethanol per 1 ml of Trizol Reagent used for the homogenization. The samples were briefly vortexed and centrifuged at 7,500 x g for 5 minutes at 4ºC. After discarding the wash, the RNA pellet was air dried for 5-10 minutes and then resuspended in 20-50 µl of RNAase-free water. Samples were incubated in a heat block set at 55-60ºC for 10-15 minutes. Concentration for subsequent use was determined using the Nanodrop and RNA was stored at -80°C until it was used for cDNA synthesis.

### *3.3.3 cDNA synthesis*

To perform the analysis of mRNA copy number, the complementary Deoxyribonucleic Acid (cDNA) was generated from RNA extracted previously, using Bio-Rad iScript cDNA synthesis kit. The RNA samples and the components of the kit were thawed over the ice and later kept on it. A master mix was prepared for n+1 samples with following components:

| Component | Volume/Reaction |
|---|---|
| 5x iScript reaction mix | 4 µl |
| iScript reverse transcriptase | 1 µl |

Volumes x and y were calculated to obtain 1 µg of total RNA in 20 µl of reaction for each sample. Later, in labeled PCR-tubes following ingredients were mixed:

| Component | Volume/Tube |
|---|---|
| Nuclease-free water | x µl |
| RNA template | y µl |
| Mastermix | 5 µl |
| Final volume | 20 µl |

The complete reaction mix was vortexed, shortly centrifuged and incubated in a thermocycler with the consecutive steps:

| | |
|---|---|
| 25ºC | 5 minutes |
| 42ºC | 30 minutes |
| 85ºC | 5 minutes |
| 4ºC | ∞ |

This way cDNA was synthesized. Then, it was 50 times diluted in double-distilled water ($_{dd}H_2O$) and stored at -20°C until it was used in qPCR.

### *3.3.4 qPCR*

The cDNA was used to perform quantitative real-time polymerase chain reaction (qPCR) with at least three technical replicates. Mastermixes were prepared for each gene with 20% excess.

| Components | Volume/Reaction |
|---|---|
| SYBR Green | 3.6 µl |
| Reverse primer (25 µM) | 0.2 µl |
| Forward primer (25 µM) | 0.2 µl |

First 4 µl/well of Mastermix were pipetted to the 384-well-plate and later 4 µl/well of cDNA were added. Before placing the plate in the qPCR machine, it was sealed and centrifuged for about 1 minute. The reaction was performed using the following qPCR protocol:

| | | |
|---|---|---|
| 95ºC | 5 minutes | |
| 95ºC | 30 seconds | |
| 60ºC | 30 seconds | x 40 |
| 72ºC | 30 seconds | |
| 95ºC | 30 seconds | |
| 60ºC | 30 seconds | |
| 72ºC | 30 seconds | |

Data were analyzed with Quant Studio™ Real-Time PCR Software.

### *3.3.5 DQ-BSA assay*

The cells were plated day before in 96 well-plate with black walls and transparent glass bottom. Each condition was tested with 24 technical replicates. The initial stock of DQ Green BSA was prepared fresh by resuspending 1 mg in 1 ml of sterile PBS. After the medium was changed to fresh one with DQ Green BSA (10 µl/ml) cells were incubated at 37°C for 1 hour. After incubation, they were washed twice with warm PBS which was replaced by 100 µl/well of EBSS medium. The plate was relocated to the plate reader and readings were taken every 5 minutes for 4 hours (excitation 505 nm and emission 515 nm). When the assay was completed, the protein concentration per well was measured applying Pierce BCA assay and used to normalize the data.

### *3.3.6 Protein concentration determination using Pierce BCA assay*

The medium was aspirated from the plate and 125 µl/well of $_{dd}H_2O$ was added. The plate was incubated for 1 hour at room temperature with mild shaking to lyse the cells. Afterwards, 100 µl of double dye working mixture were added to each well (25 Pierce BCA buffer: 1 Pierce BCA dye). After 30 minutes of incubation at 37°C, the plate was read at 562 nm in the plate reader. The results were analyzed using Microsoft Excel 2016 and protein concentration was calculated based on the calibration curve, obtained with the same kit and bovine serum albumin (BSA), and used to normalize other assays using plate reader.

### *3.3.7 FACS determinations*

Flow cytometry (FACS) was employed to determine lysosomal mass, mitochondrial superoxide levels, mass and membrane potential. In order to perform these experiments, the cells were plated in 6 cm plates, in triplicates for each condition plus the corresponding controls (at least one not stained and stained). First, the cells were washed with warm PBS and then adequate protocol was applied depending on the studied aspect.

**Lysosomal mass determination:** The medium was replaced by DMEM with 200 nM LysoTracker Green DND-26 dye and cells were incubated for 20 minutes at 37°C.

**Mitochondrial superoxide determination:** In this case, the PBS always contains 0.5 µM D-Glucose. The medium was replaced by warm PBS containing 0.5 µM D-Glucose and 5 µM MitoSOX Red dye and cells were incubated for 20 minutes at 37°C. Afterwards, positive controls with 100 µM $H_2O_2$ or 100 µM antimycine were incubated for 20 minutes at 37°C.

**Mitochondrial mass determination:** The medium was replaced by medium containing 70 nM MitoTracker Green FM dye and the cells were incubated for 25 minutes at 37°C.

**Mitochondrial membrane potential determination:** The medium was replaced by medium containing 20 µM JC-1 dye. The cells were incubated for 20 minutes at 37°C; cells incubated later for 5 minutes with 100 µM FCCP were used as positive control.

After the incubation, cells were washed twice with warm PBS, 500 µl of TrypLE Express Enzyme were added to each plate and the cells were incubated for 7 minutes at 37°C. Then, cells were collected using 1 ml of PBS to neutralize the activity of the enzyme and centrifuged for 5 minutes at 800 g and 4°C. After the supernatant was aspirated, cells were resuspended in 1 ml of cold PBS and transferred to FACS tubes. The tubes were kept on ice until the results were collected using a Calibur flow cytometer using GFP 530/30 (lysosomal mass), PI 585/42 (mitochondrial superoxide) or PE 585/42 (mitochondrial membrane potential). Data was analyzed using the DIVA software.

### *3.3.8 Mitochondrial oxygen consumption determination*

Determination of basal mitochondrial oxygen consumption was performed using Seahorse XF96 extracellular Flux Analyzer in agreement with the manufacturer's instructions. One day before, the cells were plated in a Seahorse plate (15,000 cell/well) and 200µl/well of XF Calibrant Solution were added into each well of the cartridge for hydration of the Seahorse sensor microplate. Both plates were incubated overnight at 37°C. Following day, the medium was replaced by XF assay medium (160 µl/well) and kept in Seahorse incubator at 37°C for 1 hour without $CO_2$. Following conditions were tested: standard medium used to grow cells described in *section 3.2.1*, medium with low level of glucose, medium supplemented with 2-deoxy-D-glucose to inhibit glycolysis, medium supplemented with 2-deoxy-D-glucose and pyruvate, medium supplemented with carbonyl cyanide m-chlorophenyl hydrazone (CCCP) to uncouple mitochondria and one more supplemented with DMSO as a control for CCCP. Each condition was tested with 8 technical replicates.

When the assay was completed, the amount of protein per well was measured with Pierce assay and used for normalization.

## 3.4 Protein biochemistry

### *3.4.1 Cell lysates*

The cell pellets were resuspended in an adequate volume of RIPA buffer (150 mM NaCl, 1% Triton X, 0.5% sodium deoxycholate, 0.1% SDS in 50 mM Tris, pH=8.0) with protease and phosphatase inhibitors (50-100 µl, depending on the number of cells) by pipetting. Later, the cell suspensions were transferred to 1.5 ml Eppendorf tubes and mixed by rotation at 4°C for 30 minutes. Afterwards, the tubes were centrifuged at 4°C for 30 minutes at 15,700 g and the supernatants were transferred into new 1.5 ml Eppendorf. The protein concentration was determined by Bradford Protein Assay (Bio-Rad).

### *3.4.2 Brain homogenates*

Stock solution of homogenization buffer was prepared by mixing 2 ml of 2 M NaCl, 100 µl of 0.5 M EDTA and 1 ml of 1 M HEPES pH 7.4 and topping with $_{dd}H_2O$ to final volume of 50 ml. Stock solution can be kept at 4ºC for several months. Homogenization buffer was activated by dissolving 0.08 g of protease inhibitor, 1 tablet of 5 phospho-stop phosphatase inhibitor and 0.0016 g of Dithiothreitol in 10 ml of stock solution.

Firstly, 20% SDS was warmed up. Tissue was relocated from -80°C freezer in a -20°C cool box and transferred to previously prepared 2 ml tubes with 360-1080 µl (dependently on amount of tissue) of

homogenization buffer and 3 metallic beads. Subsequently, samples were oscillated on bead mill for 1 minute at 20 Hz and quickly span-down at maximum speed for 10 s. After addition of 40-120 µl of 20% SDS, samples were oscillated again on bead mill for 1 minute at 20 Hz and quickly span-down at maximum speed for 10 s. if any visible opaque streaks or solid matter remained, oscillation and spin-down were repeated. Homogenate was mixed several times with a 27G needle in a 1 ml syringe and transferred to new tube.

### *3.4.3 Protein concentration determination using Bradford assay*

Protein concentration of cell lysates was measured using Bradford Protein Assay (Bio-Rad) in agreement with manufacturer's instructions. First, the standard curve was determined using bovine serum albumin (BSA). To assess the protein concentration in a glass tube, 1 µl of sample was mixed with 800 µl of $_{dd}H_2O$ and 200 µl of Bradford Protein Assay were added. The tubes were vortexed and incubated in the dark at room temperature for 5 minutes. The mixture was transferred into a plastic cuvette and its absorbance at 595 nm was read in duplicates using a GeneQuant 1300 spectrophotometer. Protein concentration was determined based on the standard curve and using Microsoft Excel 2016.

### *3.4.4 Protein concentration determination using Pierce BCA assay*

Protein standards were prepared using the pipet scheme provided by Thermo Scientific (A = 2000 µg/µl, B = 1500 µg/µl, C = 1000 µg/µl, D = 750 µg/µl, E = 500 µg/µl, F = 250 µg/µl, G = 125 µg/µl, H = 25 µg/µl, I = 0 µg/µl) to obtain standard curve.

Homogenates were diluted 1:40 in $_{dd}H_2O$ (3 µl in 117 µl). BCA working solution was prepared according to the instruction provided by Thermo Scientific (50 reagent A : 1 reagent B). 50 µl of diluted sample was added to 1 ml of working solution. After incubation at 37°C for 30 min the mixture was transferred into a plastic cuvette and absorbance at 562 nm was measured in duplicates using a GeneQuant 1300 spectrophotometer. Protein concentration was calculated based on the standard curve using Microsoft Excel 2016.

### *3.4.5 SDS-PAGE*

Sodium dodecyl sulfate polyacrylamide gel electrophoresis (SDS-PAGE) was applied to separate denaturized proteins with regard to their molecular weight. Gels were prepared using 40% acrylamide solution. The resolving 12% gels were buffered with Tris/HCl of pH 8.8, when the stacking 4% gels were buffered with Tris/HCl of pH 6.8. The 1 mm thick gels were prepared using the Bio-Rad system. First, the resolving part was poured between the glasses and it was topped with isopropanol to avoid air bubbles. After the gel was polymerized isopropanol was discarded, the stacking part was casted and the 10-well or 15-well comb was fitted. The complete polymerized gels were stored in a box of running buffer at 4°C or used immediately.

In order to separate proteins from lysates or homogenates with regard to their molecular weight, samples were first diluted with adequate volume of $_{dd}H_2O$ or RIPA buffer in order to load the same amount of protein in each well, then they were mixed with 6x SDS loading buffer. Samples were boiled for 5 minutes at 95ºC and cooled before loading. The electrophoresis run was performed in Mini-Protean Tetra System (Bio-Rad) with an amperage of 50 mA per pair of gels. The Page Ruler plus Prestained was used as a standard of molecular weight; the markers are visible at 250, 130, 100, 70, 55, 35, 25, 15 and 10 kDa.

### *3.4.6 Western blotting*

The transfer of separated proteins from the SDS gel into a polyvinylidene fluoride membrane (PVDF) was performed using a wet blotting system. The PVDF membranes were activated for 1 minute in pure methanol, washed with $_{dd}H_2O$ for 1 minute and equilibrated in transfer buffer for at least 5 minutes. Gels and western blot papers were also equilibrated in cold transfer buffer. Afterwards, each gel and membrane were assembled together between 4 layers of western blot papers. The transfer was performed from the gel to the PVDF membrane at 100 V for 90 minutes.

### *3.4.7 Immunostaining*

When the transfer was over, the PVDF membranes were blocked in 5% milk (blocking solution) for 1 hour with mild shaking. Subsequently, membranes were washed three times with Tris-buffered saline with Tween 20 (TBS-T) for 10 minutes and incubated in primary antibody for 1 hour at room temperature or overnight at 4°C. Following the incubation, the membranes were washed with TBS-T three times for 10 minutes at room temperature and incubated with HRP-secondary antibodies for 1 hour at room temperature. The concentration of HRP-secondary antibodies in 5% milk was 1:4,000 or 1:8,000 depending on the concentration of primary antibody. Like before, after the incubation the membranes were washed with TBS-T three times for 10 minutes at room temperature. Afterwards, membranes were incubated with Luminata Clasico Western HRP Substrate for 3 minutes and the chemiluminescence was detected using medical X-ray films and a Curix 60 processor. The films were scanned and the bands were quantified using ImageJ. Always at least 6 animals were tested.

## 3.5 Statistical analysis

The results were processed using Microsoft Excel 2016 and the values were normalized to loading control. Each time one-tailed T test for two heteroscedastic samples was applied unless stated otherwise. All the values were graphically represented with corresponding control, which was set to 1 (except for some experiments where the total number was kept); graphs were designed in GraphPad Prism 6. Asterisks in the graphs symbolize P values in a following manner:

* $P \leq 0.05$

** $P \leq 0.01$

*** $P \leq 0.001$

# 4 Results

In order to determine effects of defective endocytosis on mitochondrial function it was necessary to inspect levels of mitochondrial proteins and their gene expression in the murine brains of key endocytic mutants, endophilin-A and synaptojanin-1. Several aspects of mitochondrial function were subsequently examined in MEF isolated from mutant mice given that this clonal cell line resembles key defects studied here. Namely, mitochondrial mass, membrane potential, respiration, glycolysis and reactive oxygen species production were assessed. Moreover, lysosomal mass and proteolytic activity were measured in MEF to characterize condition of lysosomes that may affect fitness of mitochondria. Functional iron metabolism was studied in both MEF and brains of endophilin-A triple knock-out. Furthermore, PI3K/AKT/mTOR pathway was examined in endophilin-A triple knock-out.

## 4.1 Statistical analysis of next generation sequencing data

Phenotypes of mice having the following genotypes were under research: endophilin-A double knock-out, endophilin-A triple knock-out (TKO), synaptojanin-1 knock-out (KO). C57BL/6J wild type and synaptojanin-1 wild type mice were used as control for endophilin-A TKOs and synaptojanin-1 KOs, respectively. Brains of newborn mice (p0) of synaptojanin-1 wild type (SYNJ1 WT), synaptojanin-1 knock-out (SYNJ1 KO), C57BL/6J wild type (BL6 WT) and endophilin-A triple knock-out (EndoA123 TKO) and brains of 14 days old pups (p14) of C57BL/6J wild type (BL6 WT) and endophilin-A double knock-out (EndoA12 DKO) were collected, RNA was extracted from their hippocampi and used to perform Next-Generation Sequencing (NGS). Statistical analysis of NGS data shows that knock-out of endocytic proteins synaptojanin-1 as well as endophilin-A leads to overall downregulation of the expression of mitochondrial genes in the hippocampus. By comparing the expression of the whole mitochondrial gene list between each KO and the respective control, using Student's T-test followed by Bonferroni multi-test correction, it could be confirmed that knock-out significantly affects the pool of mitochondrial genes as a whole (Figures 4.1 and 4.2). To control if this was a specific issue for mitochondria or also observed with other organelles, gene lists for lysosomes, peroxisomes, Golgi and endoplasmic reticulum (ER) were also considered. In the hippocampus of synaptojanin-1 and endophilin-A knock-out mice additional downregulation of Golgi-related genes expression was detected, hence, it is interesting potential future direction of the research to study how knock-out of synaptojanin-1 affect structure and function of Golgi.

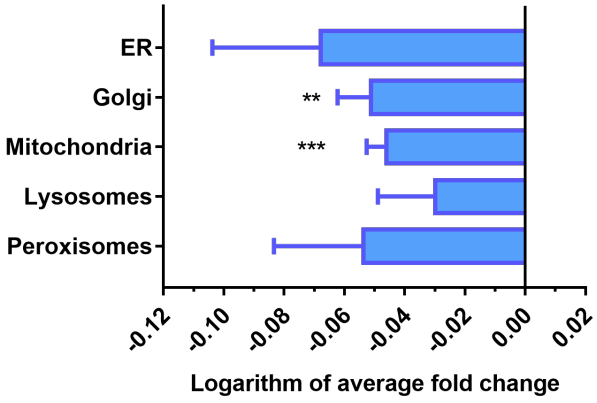


*Figure 4.1 Average fold change (logarithm transformed) of expression of genes specific for given organelle observed in the hippocampi of endophilin-A triple knock-out (EndoA123 TKO) p0 mice in comparison to black 6 wild type (BL6 WT). ** $P \leq 0.01$, *** $P \leq 0.001$ from T-test with Bonferroni multi-test correction.*

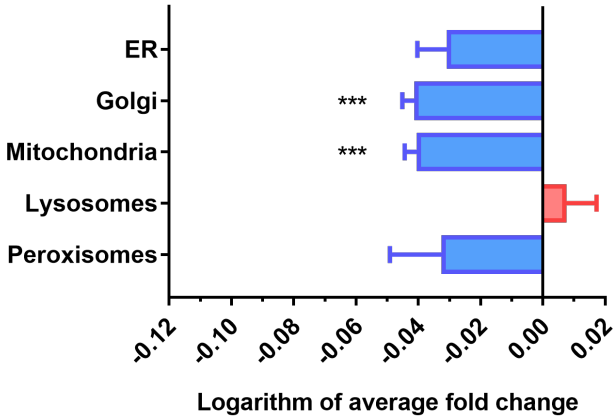


*Figure 4.2 Average fold change (logarithm transformed) of expression of genes specific for given organelle observed in the hippocampi synaptojanin-1 knock-out (SYNJ1 KO) in comparison to of synaptojanin-1 wild type (SYNJ1 WT). *** $P \leq 0.001$ from T-test with Bonferroni multi-test correction.*

When looking at the expression of hundreds of genes as a group, as it occurs for the organelle gene lists, it is important to determine whether the effect observed is due to consistent changes across many genes, or if it is the result of strong changes in few genes that skew the group. Thus, the number of genes with significantly changed expression was subject to analysis. According to NGS data, expression of numerous mitochondrial genes is significantly changed due to knock-out of synaptojanin-1 or endophilin-A (Figure 4.3): 327 of 905 in endophilin-A double knock-out (EndoA12 DKO), 228 of 898 in endophilin-A triple knock-out (EndoA123 TKO), both in comparison to C57BL/6J wild type (BL6 WT) and 51 in 907 in synaptojanin-1 knock-out (SYNJ1 KO) normalized to synaptojanin-1 wild type (SYNJ1 WT). Number of differently expressed mitochondrial genes detected in EndoA12 DKO is higher than one detected in EndoA123 TKO most likely due to the fact that EndoA12 DKO mice were collected after 14 postnatal days after birth when the impact of defective endocytosis on mitochondrial transcripts may be stronger than in newborn mice.

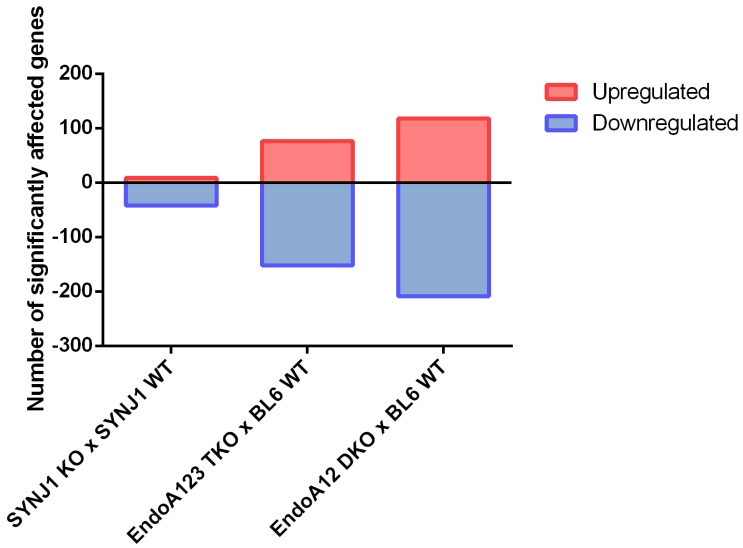


*Figure 4.3 Number of mitochondrial genes which expression was significantly affected by knock-out of endocytic proteins: synaptojanin-1 (SYNJ1), endophilin-A triple knock-out (EndoA123 TKO) and endophilin-A double knock-out (EndoA12 DKO).*

Importantly, the vast majority of genes with differential expression were down-regulated, which explains why the overall gene list was showing a decrease in the endocytic mutants compared to the respective controls. Moreover, pathway analysis of the transcriptional signatures of EndoA123 TKO hippocampi, performed using the Ingenuity Pathway Analysis (IPA; Qiagen) software, indicates that one of the most significantly enriched pathways is mitochondrial dysfunction [23]. Similarly, pathway analysis of the transcriptional signatures of synaptojanin-1 knock-out (SYNJ1 KO) cortexes and hippocampi, also completed with IPA, shows that mitochondrial dysfunction is one of the ten most significantly enriched pathways based on Fisher exact test p values (x axis) which are presented in Figure 4.4.

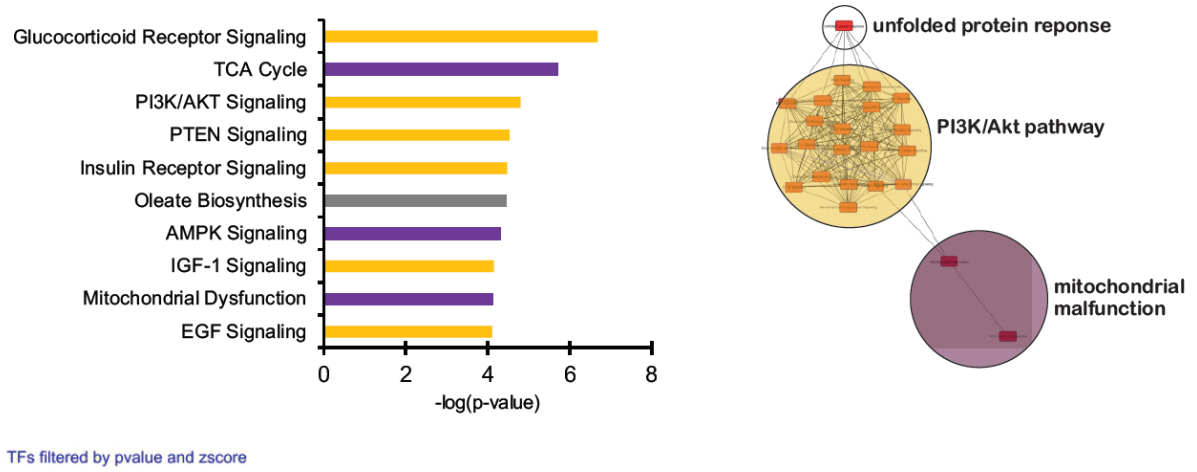


*Figure 4.4 Pathway analysis of the transcriptional signatures of synaptojanin-1 knock-out (SYNJ1 KO) hippocampi. The color coding refers to pathways that are represented by a similar group of genes. In yellow, the pathways that scored significantly mostly due to PI3K pathway. In purple, the pathways that scored due to mitochondrial respiratory chain/OXPHOS genes. The same colors are employed in the right side of the image, to illustrate how the different pathways are related to each other. Two major nodes are evident, one centered around the PI3K pathway and the other around mitochondrial genes.*

## 4.2 Mitochondrial dysfunction

### *4.2.1 Mitochondrial mass and biogenesis*

It was observed that fluctuations of the protein levels of known mitochondrial biogenesis regulators do not represent any specific trend such as global decrease or increase, suggesting that knock-out of endophilin-A (Figure 4.5) or synaptojanin-1 (Figure 4.6) does not affect mitochondrial mass in general. Mitochondrial import receptor subunit TOM20 (TOMM20) was used as indicator of mitochondrial mass. Following mitochondrial biogenesis regulators were tested: NAD-dependent protein deacetylase sirtuin-1 (SIRT1), peroxisome proliferator activated receptor gamma coactivator 1 alpha (PGC1A), nuclear respiratory factor 1 (NRF1), nuclear factor erythroid-derived 2-like 2 (NRF2), mitochondrial transcription factor A (TFAM). Protein levels were measured in p0 brains and MEF by *western* blot as described in *Methods*.

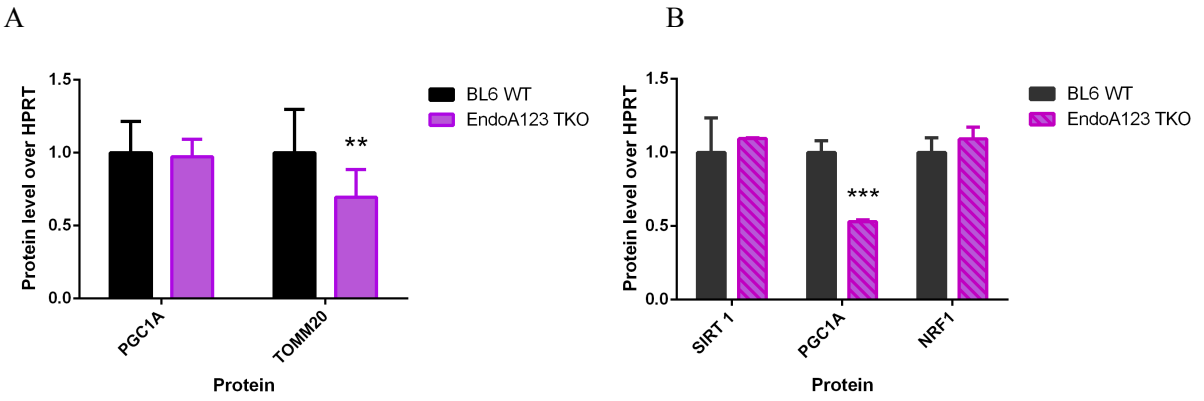


*Figure 4.5 Mitochondrial biogenesis regulators and mass indicator (TOMM20) detected by western blot in C57BL/6J wild type (BL6 WT) and endophilin-A triple knock-out (EndoA123 TKO) mouse p0 brains on the left (A) and MEF on the right (B). * P ≤ 0.05, ** P ≤ 0.01, *** P ≤ 0.001 from T-test.*

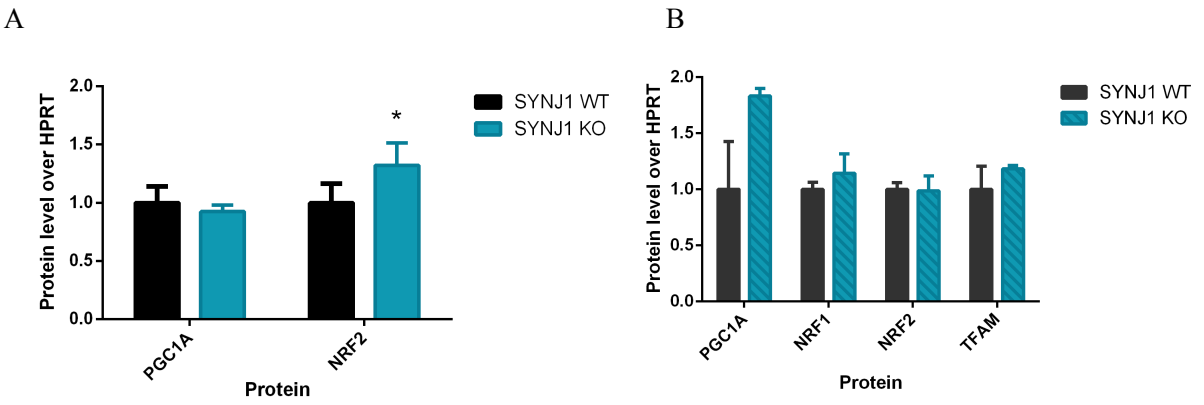


*Figure 4.6 Mitochondrial biogenesis regulators detected by western blot in in synaptojanin-1 wild type (SYNJ1 WT) and synaptojanin-1 knock-out (SYNJ1 KO) mouse p0 brains on the left (A) and MEF on the right (B). * P ≤ 0.05, ** P ≤ 0.01, *** P ≤ 0.001 from T-test.*

Mitochondrial mass was measured by a flow cytometer, as detailed in *Methods*, using MitoTracker Green dye which is insensitive to changes in mitochondrial membrane potential. Expectedly, the data confirm that mitochondrial mass is not significantly altered due to knock-out of endocytic proteins endophilin-A (Figure 4.7) or synaptojanin-1 (Figure 4.8). Given that the transcriptional program of mitochondrial biogenesis is repressed, the unaltered mitochondrial mass is likely a consequence of a decrease in the degradation of mitochondria. This process is dependent on autophagy, which is impaired in the endophilin mutants [23].

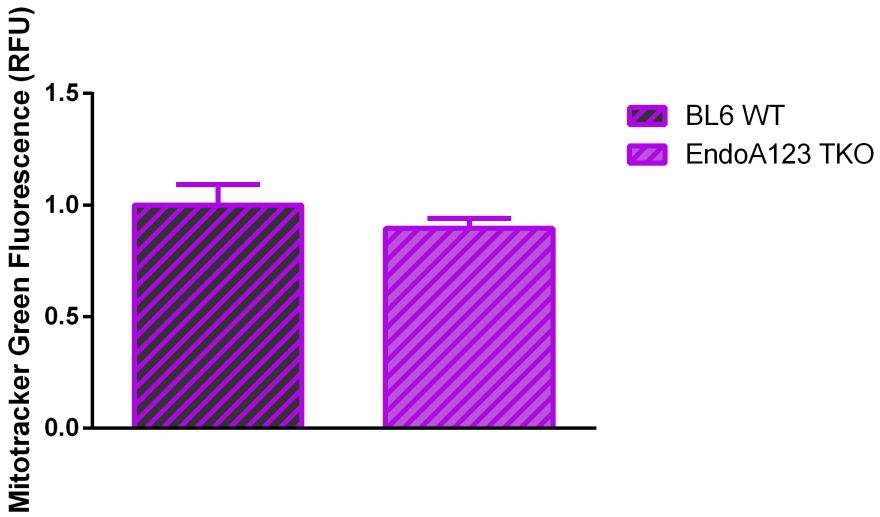


*Figure 4.7 Mitochondrial mass measured by FACS in C57BL/6J wild type (BL6 WT) and endophilin-A triple knock-out (EndoA123 TKO) MEF using LysoTracker Green and normalized to WT control.*

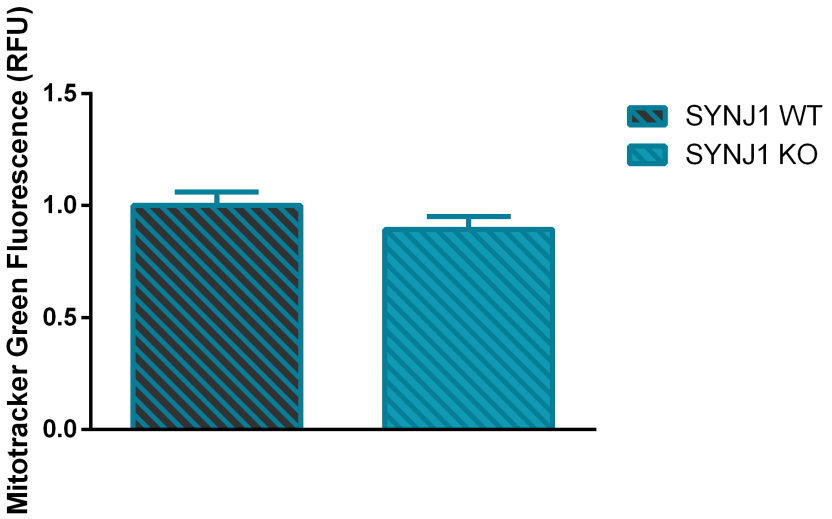


*Figure 4.8 Mitochondrial mass measured by FACS in synaptojanin-1 wild type (SYNJ1 WT) and synaptojanin-1 knock-out (SYNJ1 KO) MEF using LysoTracker Green and normalized to WT control.*

### *4.2.2 Membrane potential*

Membrane potential was measured using a flow cytometer, as detailed in *Methods*, and the raw data were analysed using DIVA software (manufacturer). These measurements show that knock-out of endophilin-A in brain causes a decrease in mitochondrial membrane potential, (Figure 4.9) which is a strong indicator of impaired mitochondrial function. Similarly, reduced mitochondrial membrane potential was observed in fibroblasts missing synaptojanin-1 alleles (Figure 4.10).

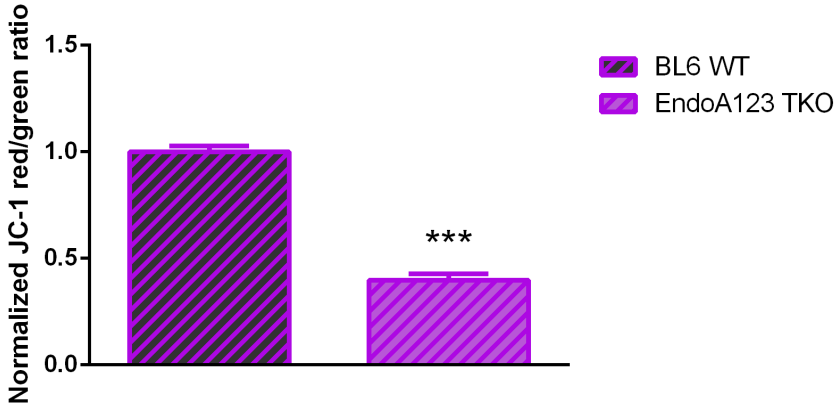


*Figure 4.9 Mitochondrial membrane potential measured by FACS in C57BL/6J wild type (BL6 WT) and endophilin-A triple knock-out (EndoA123 TKO) MEF using JC-1 and normalized to WT control. *** $P \leq 0.001$ from T-test.*

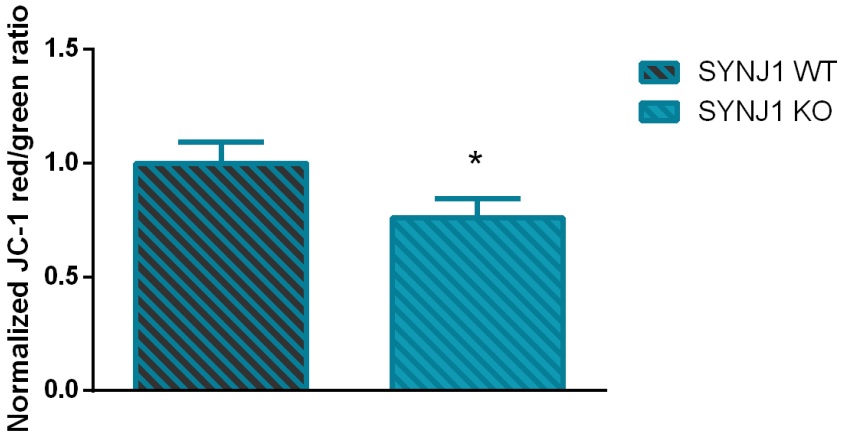


*Figure 4.10 Mitochondrial membrane potential measured by FACS in synaptojanin-1 wild type (SYNJ1 WT) and synaptojanin-1 knock-out (SYNJ1 KO) MEF using JC1 and normalized to WT control. * $P \leq 0.05$ from T-test.*

### *4.2.3 Respiration*

Not only expression of respiratory chain genes is mostly downregulated due to knock-out of endophilin-A or synaptojanin-1 but also levels of some proteins measured by *western* blot are significantly altered. Figure 4.11 is a heatmap presenting fold change of gene expression of respiratory chain proteins. In all three studied conditions: endophilin-A double knock-out (EndoA12 DKO), endophilin-A triple knock-out (EndoA123 TKO), both in comparison to C57BL/6J wild type (BL6 WT), and synaptojanin-1 knock-out (SYNJ1 KO), which was normalized to synaptojanin-1 wild type (SYNJ1 WT), big variations were detected. Observed changes are not specific to any complex of respiratory chain and do not always present the same trend in all three conditions under research. Nevertheless, the data clearly indicate that knock-out of endocytic proteins, endophilin-A or synaptojanin-1 strongly affects gene expression of respiratory chain proteins.

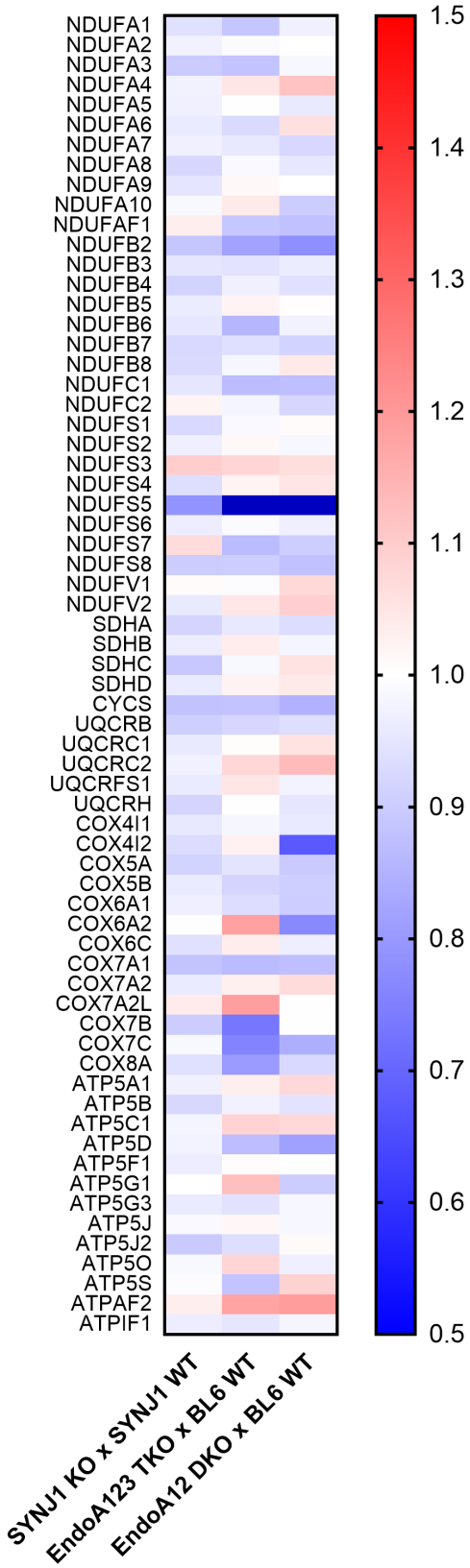


*Figure 4.11 Heatmap presenting fold change of gene expression of respiratory chain proteins sorted by complex basing on NGS data. Fold change equal to 1.0 (white) corresponds to no change in gene expression, fold change smaller than 1.0 (shades of blue) – reduced gene expression, and fold change bigger than 1.0 (shades of red) – increased gene expression.*

Furthermore, levels of oxidative phosphorylation proteins also do not follow any explicit trend such as down- or up-regulation. Following proteins were tested: NADH dehydrogenase [ubiquinone] 1 beta subcomplex subunit 8 from complex I (NDUFB8), iron-sulfur subunit of complex II (SDHB), cytochrome b-c1 complex subunit 2 from complex III (UQCRC2), cytochrome c oxidase subunit 1 from complex IV (MTCO1), ATP synthase subunit alpha from complex V (ATP5A). Significant increase in ATP5A level in endophilin-A triple knock-out (EndoA123 TKO) may be attributed to the distinctness of complex V among other respiratory chain complexes but may be also coincidental. Since the inner mitochondrial membrane encompasses the respiratory chain and oxidative phosphorylation machineries (Mitchell, 1961; Mitchell and Moyle, 1967) levels of oxidative phosphorylation proteins can be also interpreted as indicators of mitochondrial mass. Consistently with results presented in *4.2.1 Mitochondrial mass and biogenesis*, the data show that mitochondrial mass is not significantly changed because of the knock-out of endocytic proteins endophilin-A (Figure 4.12) or synaptojanin-1 (Figure 4.14). Levels of proteins were measured by *western* blot as described in *Methods*.

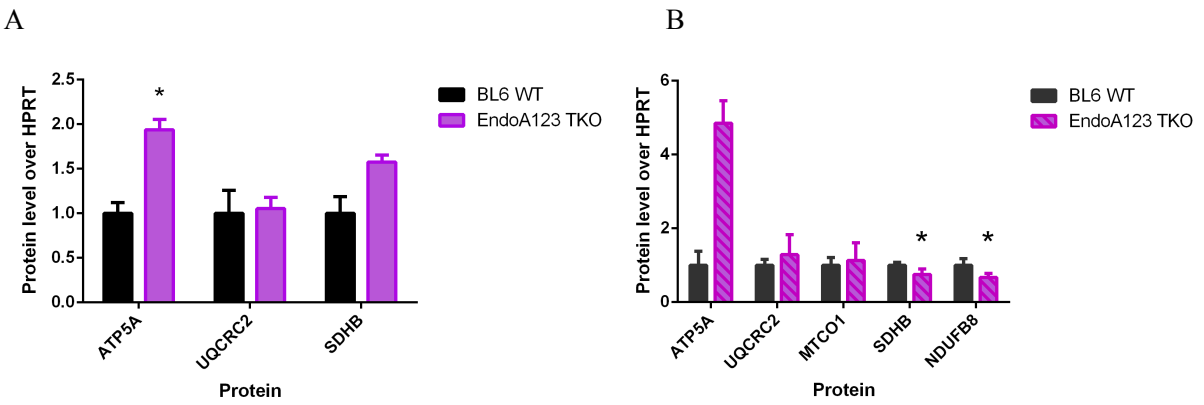


*Figure 4.12 Levels of oxidative phosphorylation proteins detected by western blot in C57BL/6J wild type (BL6 WT) and endophilin-A triple knock-out (EndoA123 TKO) p0 brains on the left (A) and MEF on the right (B). * $P \leq 0.05$ from T-test.*

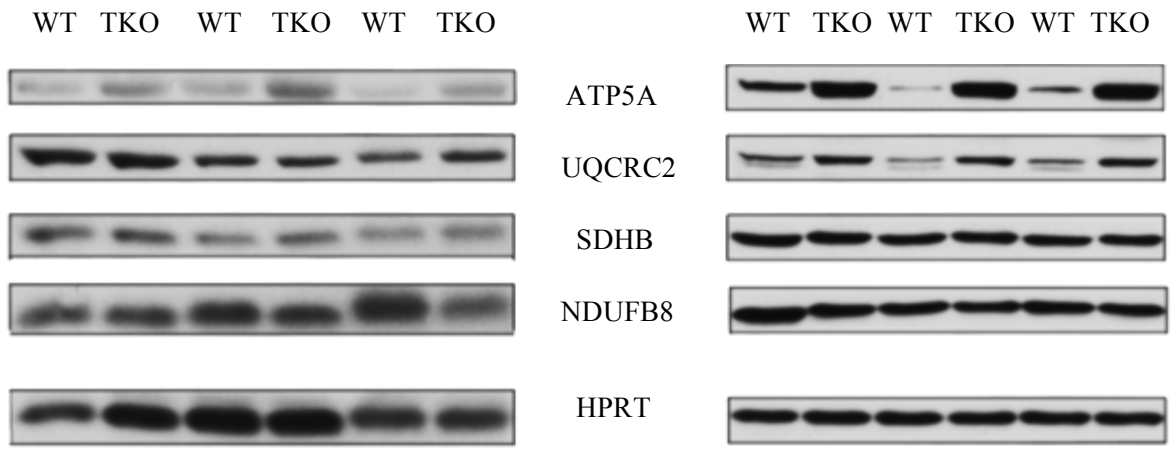


*Figure 4.13 Exemplary blots indicating levels of oxidative phosphorylation proteins detected in C57BL/6J wild type (BL6 WT) and endophilin-A triple knock-out (EndoA123 TKO) p0 brains on the left and MEF on the right).*

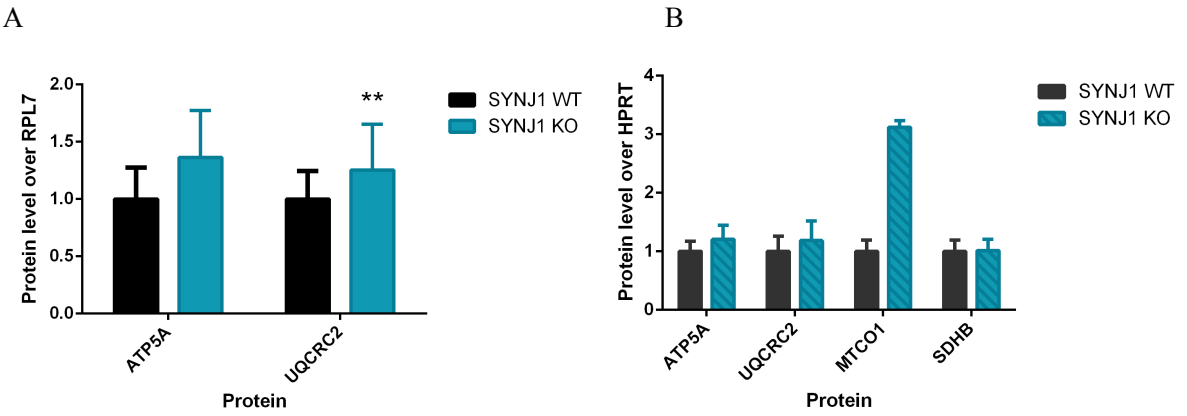


*Figure 4.14 Levels of oxidative phosphorylation proteins detected by western blot in synaptojanin-1 wild type (SYNJ1 WT) and synaptojanin-1 knock-out (SYNJ1 KO) p0 brains on the left (A) and MEF on the right (B). ** $P \leq 0.01$ from T-test.*

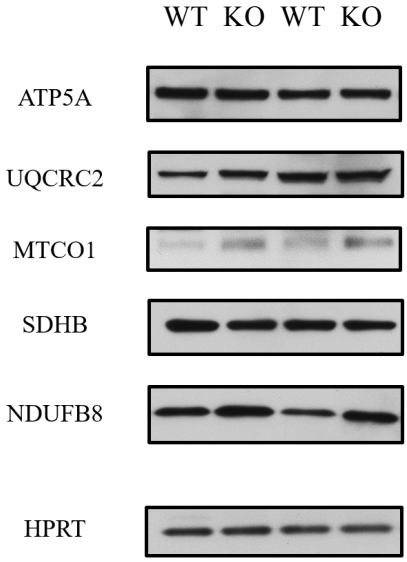


*Figure 4.15 Exemplary blots indicating levels of oxidative phosphorylation proteins detected in synaptojanin-1 wild type (SYNJ1 WT) and synaptojanin-1 knock-out (SYNJ1 KO) MEF.*

Moreover, lack of endophilin-A or synaptojanin-1 results in decreased oxygen consumption rate which was measured by Seahorse as designated in *Methods*. Since this experiment is carried out using cells as a whole, seeded in a plate, it is not possible to distinguish if the mitochondrial oxygen consumption rate is affected for example by the glycolytic rate. Thus, it is important to also supply pyruvate to the cells, so that the readout of the TCA cycle/respiratory chain is independent of glycolysis. Supplementation with pyruvate increased, but did not bring oxygen consumption rate to normal level in endophilin-A triple knock-out (Figure 4.16) and synaptojanin-1 knock-out MEF (Figure 4.18). The defects persist in the endocytic mutants even when glycolysis is inhibited by 2-deoxy-D-glucose and pyruvate is supplied. Thus, an inability to make pyruvate is not a main cause of reduced mitochondrial OCR what suggests presence of defect intrinsic to mitochondria. Nevertheless, the increase in OCR upon pyruvate supplementation also suggests that the glycolytic pathway in the mutants is not functioning optimally. Mitochondrial uncoupling using Carbonyl cyanide m-chlorophenyl hydrazone (CCCP) did not bring oxygen consumption rate to normal level in endophilin-A triple knock-out MEF what can be seen in Figure 4.17.

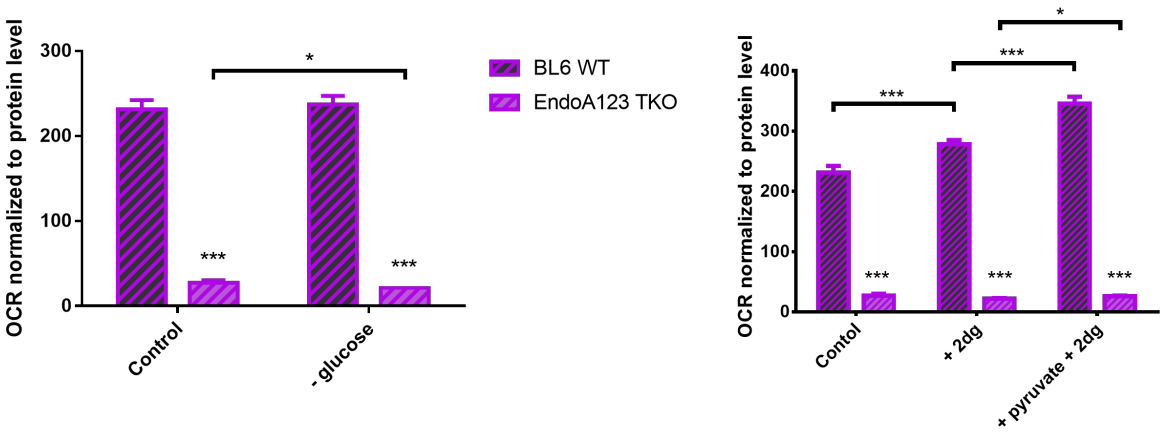


*Figure 4.16 Oxygen consumption rate measured in C57BL/6J wild type (BL6 WT) and endophilin-A triple knock-out (EndoA123 TKO) MEF in various conditions related to glycolysis. * P ≤ 0.05, *** P ≤ 0.001 from T-test*

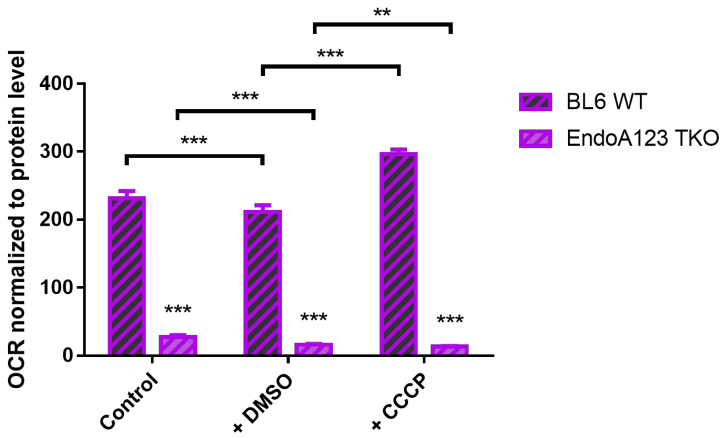


*Figure 4.17 Oxygen consumption rate measured in C57BL/6J wild type (BL6 WT) and endophilin-A triple knock-out (EndoA123 TKO) MEF after inhibition of oxidative phosphorylation and in control conditions. ** P ≤ 0.01, *** P ≤ 0.001 from T-test.*

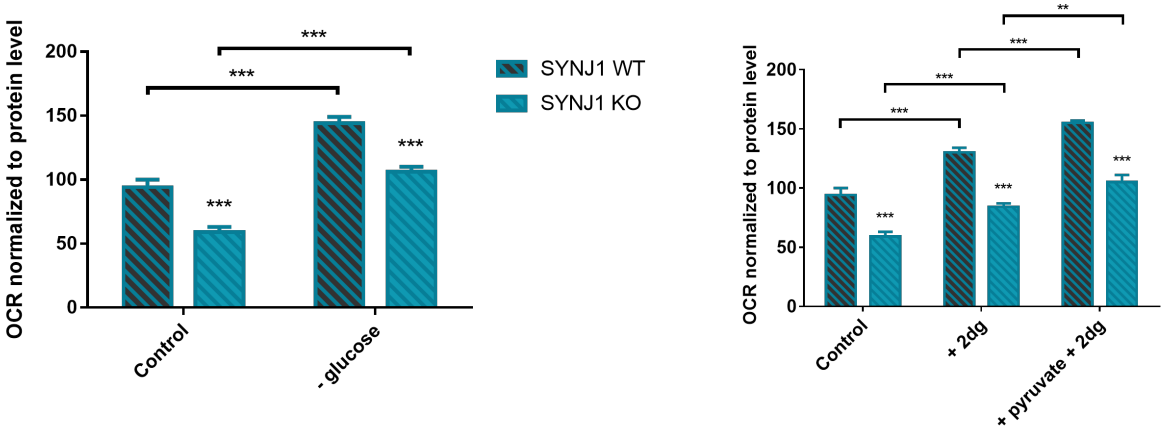


*Figure 4.18 Oxygen consumption rate measured in synaptojanin-1 wild type (SYNJ1 WT) and synaptojanin-1 knock-out (SYNJ1 KO) MEF in various conditions related to glycolysis. ** P ≤ 0.01, *** P ≤ 0.001 from T-test.*

### *4.2.4 Glycolysis*

Such greatly decreased oxygen consumption rate cannot be fully explained by only slight disturbances in glycolysis at both, gene expression and protein levels which were measured by western blot as described in *Methods*. Figure 4.19 is a heatmap presenting fold change of gene expression of glycolysis related proteins. In all three studied conditions: endophilin-A double knock-out (EndoA12 DKO), endophilin-A triple knock-out (EndoA123 TKO), both in comparison to C57BL/6J wild type (BL6 WT), and synaptojanin-1 knock-out (SYNJ1 KO), which was normalized to synaptojanin-1 wild type (SYNJ1 WT), alterations were detected. Gene expression of proteins related to glycolysis in studied knock-outs is mostly decreased and observed changes are not specific for any of the steps of glycolysis.

While OCR is substantially decreased in both, endophilin-A triple knock-out (EndoA123 TKO) and synaptojanin-1 knock-out (SYNJ1 KO) MEF there is no consistent trend in levels of glycolytic enzymes that could serve as an explanation for possible differences in glycolytic activity. This further supports the idea that defect is not extrinsic, but intrinsic to mitochondria. Discrepancies between protein levels of glycolytic enzymes detected in mice p0 brains and MEF (Figures 4.20 and 4.22) may result from combination of several factors, such as differences between applied in vitro and in vivo models, between studied tissues and their sources of nutrients. As glycolysis is not a reason for low OCR such inconsistencies are irrelevant for the previous section.

Following proteins were tested: hexokinase 1 (HK1), hexokinase 2 (HK2), pyruvate kinase isoforms (PKM2, PKM1/2), lactate dehydrogenase A (LDHA), pyruvate dehydrogenase (PDH). Levels of proteins were measured by *western* blot as detailed in *Methods*.

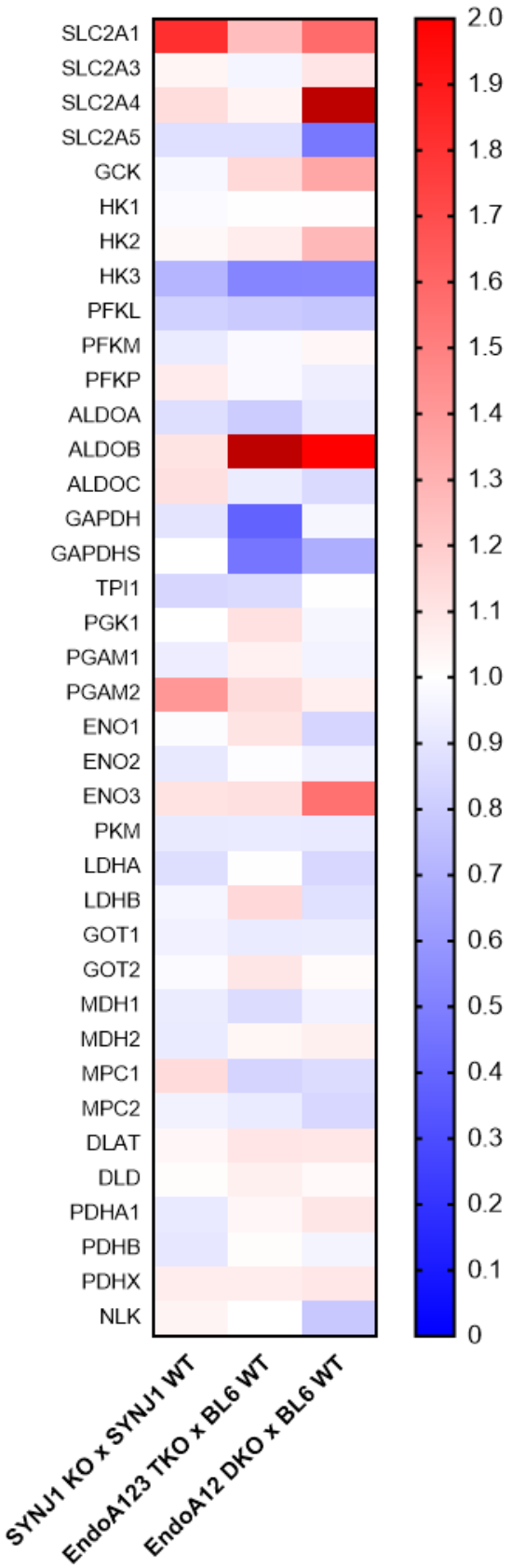


*Figure 4.19 Heatmap presenting fold change of gene expression of proteins related to glycolysis sorted by function basing on NGS data. Fold change equal to 1.0 (white) corresponds to no change in gene expression, fold change smaller than 1.0 (shades of blue) – reduced gene expression, and fold change bigger than 1.0 (shades of red) – increased gene expression.*

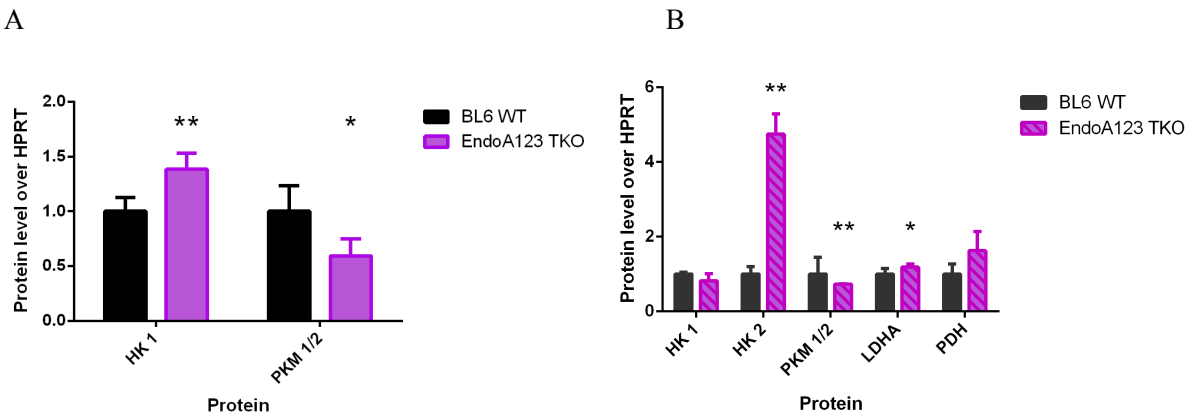


*Figure 4.20 Levels of glycolytic enzymes detected by western blot in C57BL/6J wild type (BL6 WT) and endophilin-A triple knock-out (EndoA123 TKO) p0 brains on the left (A) and MEF on the right (B). * P ≤ 0.05, ** P ≤ 0.01 from T-test.*

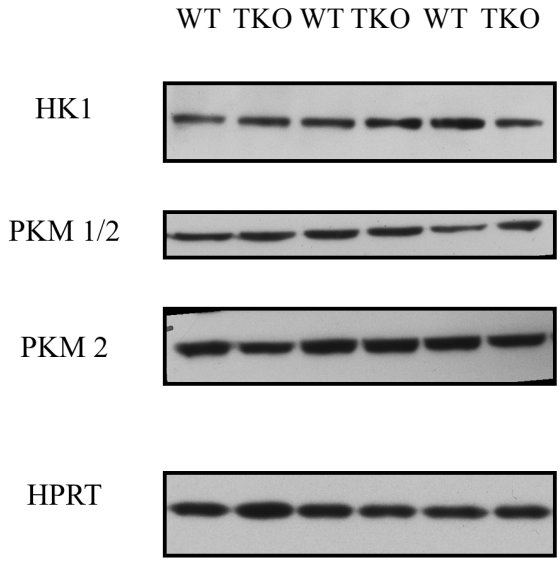


*Figure 4.21 Exemplary blots indicating levels of glycolytic enzymes detected in C57BL/6J wild type (BL6 WT) and endophilin-A triple knock out (EndoA123 TKO) p0 brains.*

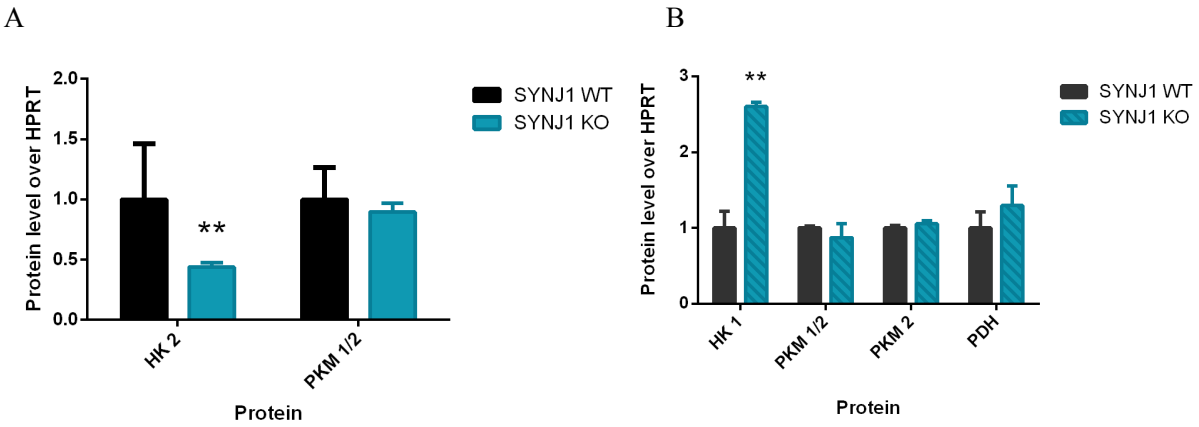


*Figure 4.22 Levels of glycolytic enzymes detected by western blot in synaptojanin-1 wild type (SYNJ1 WT) and synaptojanin-1 knock-out (SYNJ1 KO) p0 brains on the left (A) and MEF on the right (B). * P ≤ 0.05, ** P ≤ 0.01 from T-test.*

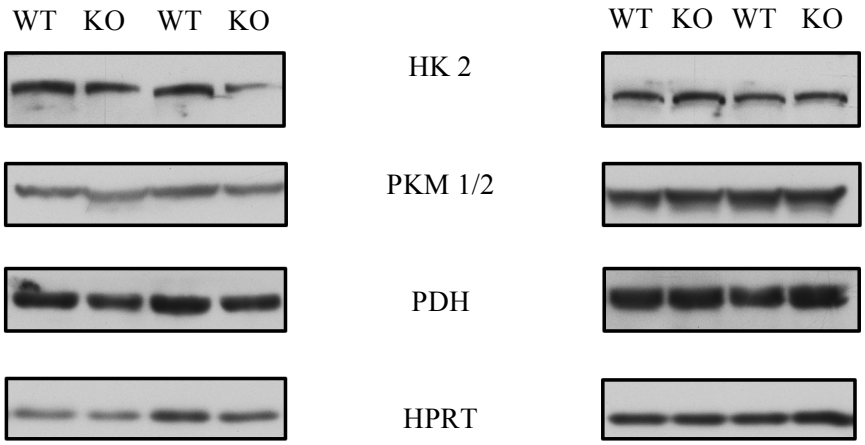


*Figure 4.23 Exemplary blots indicating levels of glycolytic enzymes detected in synaptojanin-1 wild type (SYNJ1 WT) and synaptojanin-1 knock-out (SYNJ1 KO) p0 brains on the left and MEF on the right).*

### *4.2.5 ROS production*

Superoxide levels in mouse embryonic fibroblasts were measured using a flow cytometer as detailed in *Methods*. Significantly increased superoxide levels due to knock-out of endophilin-A (Figure 4.24) show elevated ROS production which in turn is indicator of mitochondrial malfunction.

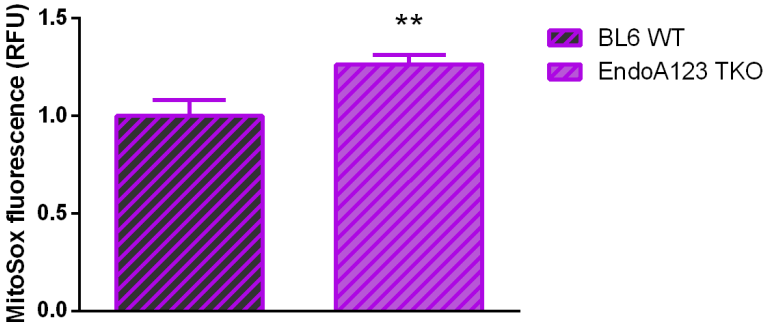


*Figure 4.24 Mitochondrial superoxide levels measured in C57BL/6J wild type (BL6 WT) and endophilin-A triple knock-out (EndoA123 TKO) MEF. ** $P \leq 0.01$ from T-test.*

Interestingly, such significant elevation of superoxide levels was not detected in synaptojanin-1 knock-out MEF (Figure 4.25).

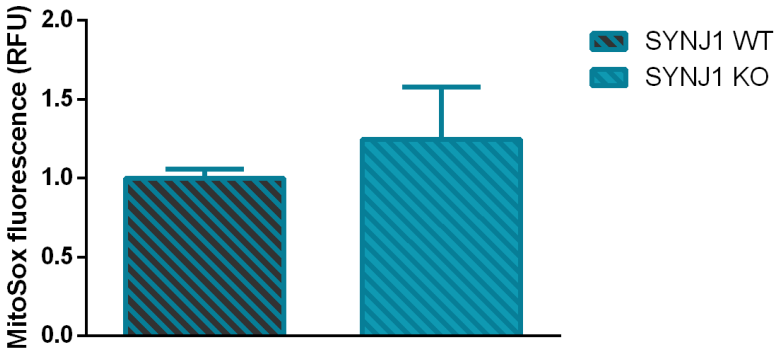


*Figure 4.25 Mitochondrial superoxide levels measured in synaptojanin-1 wild type (SYNJ1 WT) and synaptojanin-1 knock-out (SYNJ1 KO) MEF.*

## 4.3 Lysosomal dysfunction

Data obtained with flow cytometry suggest that knock-out of endocytic proteins, especially endophilin-A (Figure 4.26) but also synaptojanin-1 (Figure 4.27), results in increased lysosomal mass. The increase in LysoTracker staining is an indicator of increased lysosomal mass, but may also be affected by variation in the volume of endosomal compartments. Therefore, further experiments will be required (e.g., imaging with markers specific for lysosomes, late endosomes, early endosomes) to specify the organelle that is leading to increase in LysoTracker intensity.

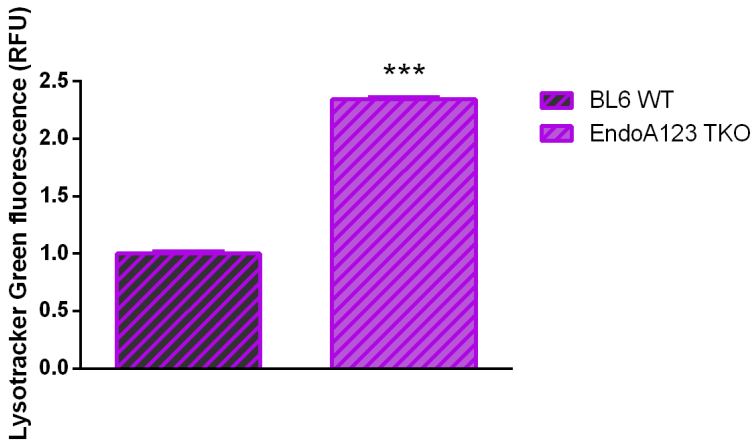


*Figure 4.26 Lysosomal mass measured in endophilin-A triple knock-out (EndoA123 TKO) MEF normalized to C57BL/6J wild type (BL6 WT) MEF. *** $P \leq 0.001$ from T-test.*

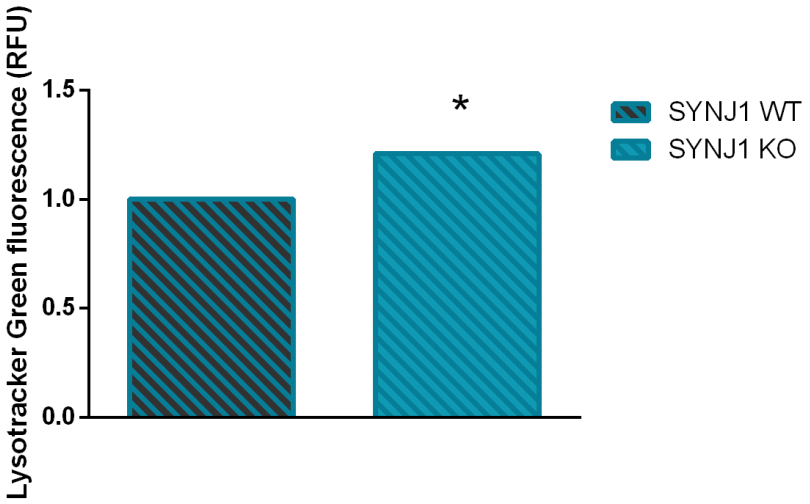


*Figure 4.27 Lysosomal mass measured in synaptojanin-1 knock-out (SYNJ1 KO) MEF normalized to synaptojanin-1 wild type (SYNJ1 WT) MEF. * $P \leq 0.05$ from T-test.*

### *4.3.1 Proteolytic activity*

Lysosomal proteolytic activity was measured with DQ BSA as described in *Methods*. Even though number or/and volume of lysosomes is likely increased, their proteolytic activity is significantly lower; principally in endophilin-A triple knock-out MEF, in which lysosomal proteolytic activity is reduced by around 40% (Figure 4.28), but also in synaptojanin-1 knock-out MEF (Figure 4.29). Bigger lysosomal mass and decreased proteolytic activity are characteristic for lysosomal malfunction.

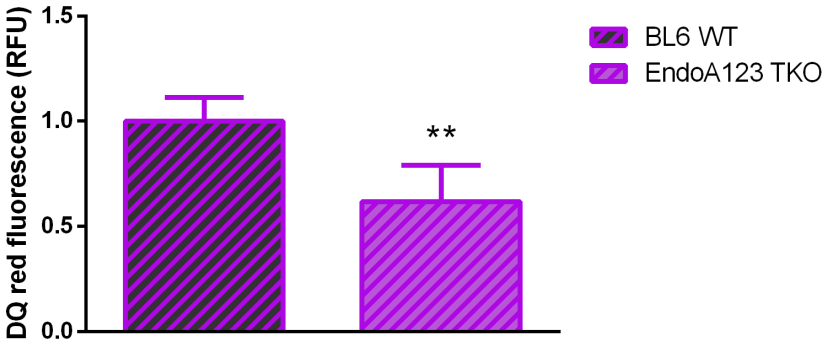


*Figure 4.28 Mean slope of proteolytic activity in endophilin-A triple knock-out (EndoA123 TKO) MEF normalized to C57BL/6J wild type (BL6 WT). ** $P \leq 0.01$ from T-test.*

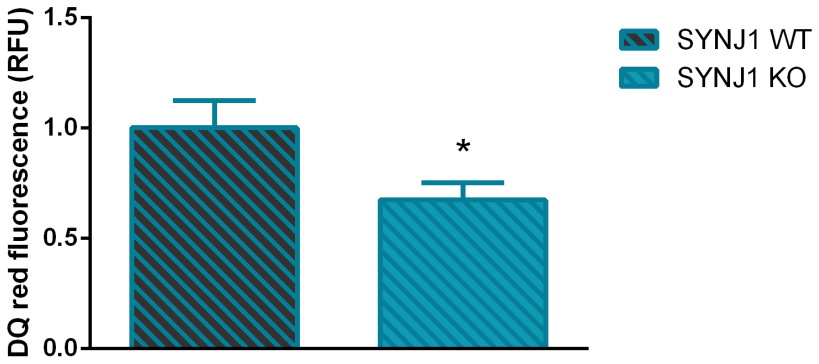


*Figure 4.29 Mean slope of proteolytic activity in synaptojanin-1 knock-out (SYNJ1 KO) MEF normalized to synaptojanin-1 wild type (SYNJ1 WT). * $P \leq 0.05$ from T-test.*

## 4.4 Functional iron deficiency

Both, statistical analysis of NGS data and levels of proteins tightly related to iron metabolism suggest that knock-out of endophilin-A results in functional iron deficiency in both, mouse p0 brains and MEF (Figure 4.31). Figure 4.30 is a heatmap presenting fold change of gene expression of proteins related to iron metabolism. In all three conditions under research: endophilin-A double knock-out (EndoA12 DKO), endophilin-A triple knock-out (EndoA123 TKO), both in comparison to C57BL/6J wild type (BL6 WT), and synaptojanin-1 knock-out (SYNJ1 KO), which was normalized to synaptojanin-1 wild type (SYNJ1 WT), strong deviations were observed. Expression of following genes was strikingly affected: ferroportin 1 (SLC40A1) which is responsible for iron export, STEAP3 Metalloreductase (STEAP3) which reduces ferric ion [$Fe^{3+}$] to ferrous ion [$Fe^{2+}$], and transferrin receptor (TFRC).

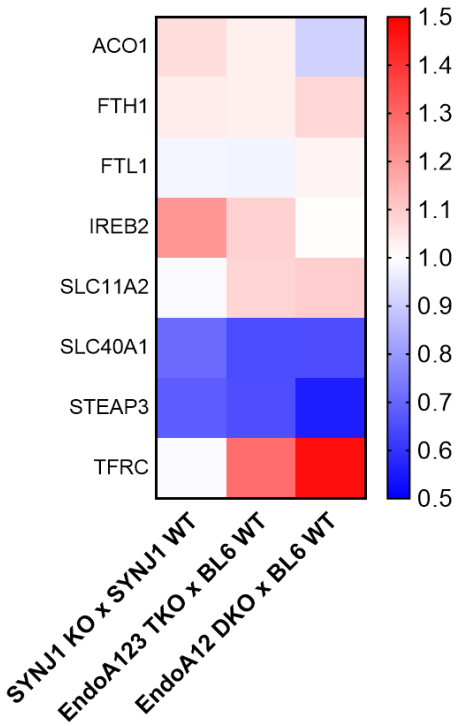


*Figure 4.30 Heatmap presenting fold change of gene expression of proteins related to iron metabolism. Fold change equal to 1.0 (white) corresponds to no change in gene expression, fold change smaller than 1.0 (shades of blue) – reduced gene expression, and fold change bigger than 1.0 (shades of red) – increased gene expression.*

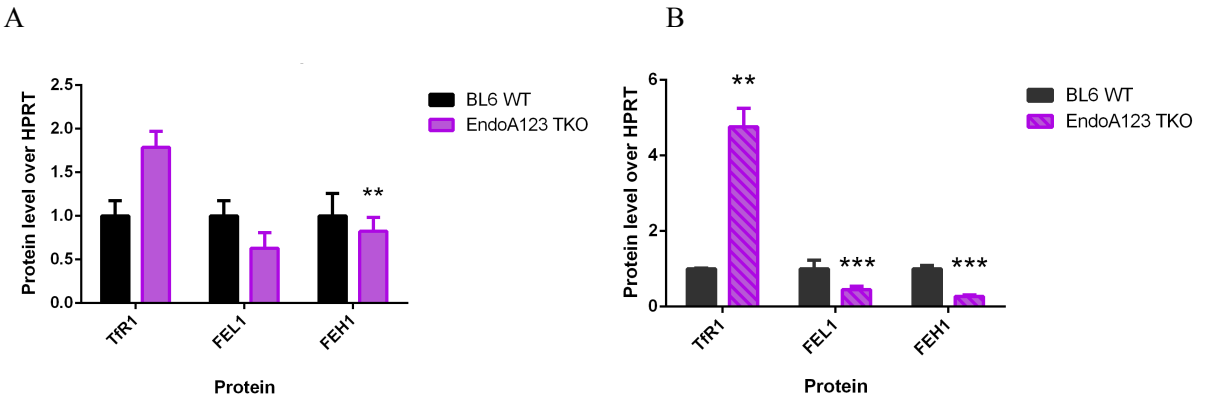


*Figure 4.31. Levels of proteins related to iron metabolism detected by western blot in C57BL/6J wild type (BL6 WT) and endophilin-A triple knock-out (EndoA123 TKO) p0 brains on the left (A) and MEF on the right (B). * $P \leq 0.05$, ** $P \leq 0.01$, *** $P \leq 0.001$ from T-test.*

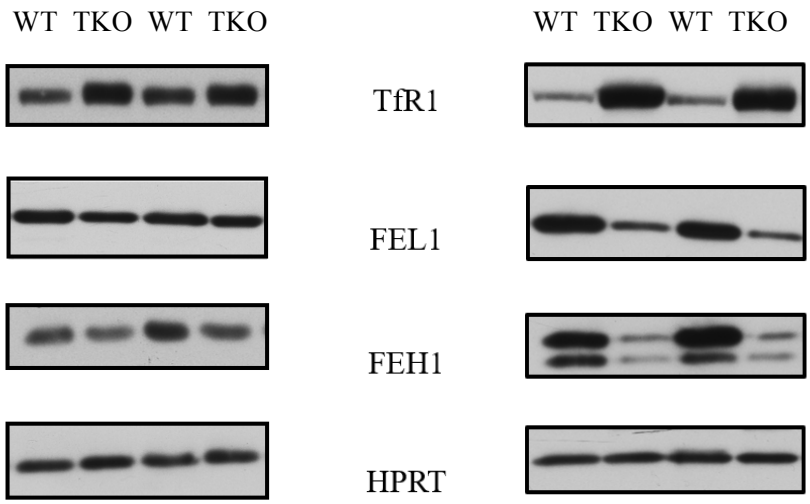


*Figure 4.32 Exemplary blots indicating levels of proteins related to iron metabolism detected by in C57BL/6J wild type (BL6 WT) and endophilin-A triple knock-out (EndoA123 TKO) p0 brains on the left and MEF on the right.*

Following proteins were tested: transferrin receptor protein 1 (TfR1), Ferritin light chain 1 (FEL1), Ferritin heavy chain 1 (FEH1). Ferritin is the key intracellular iron storage protein in both, prokaryotes and eukaryotes. Changes in levels of these proteins present similar trend in synaptojanin 1 knock-out mouse p0 brains and MEF, however, only reduction of ferritin heavy chain at protein level is statistically significant (Figure 4.33). Protein levels were detected by *western* blot as described in *Methods*.

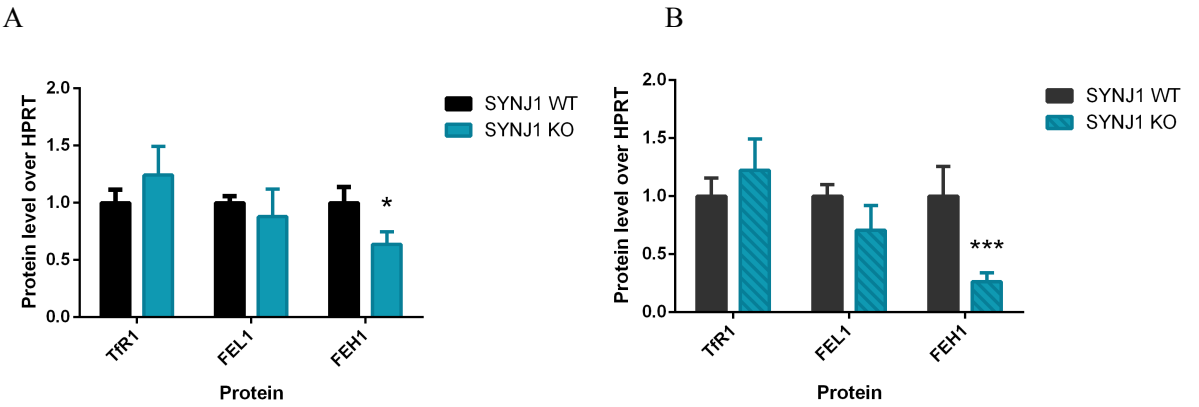


*Figure 4.33 Levels of proteins related to iron metabolism detected by western blot in synaptojanin-1 wild type (SYNJ1 WT) and synaptojanin-1 knock-out (SYNJ1 KO) p0 brains on the left (A) and MEF on the right (B). * $P \leq 0.05$, *** $P \leq 0.001$ from T-test.*

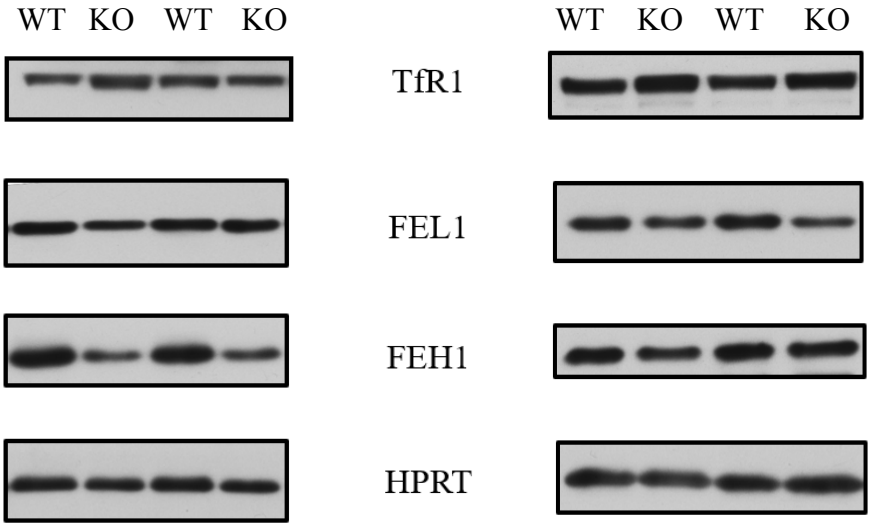


*Figure 4.34 Exemplary blots indicating levels of proteins related to iron metabolism detected in synaptojanin-1 wild type (SYNJ1 WT) and synaptojanin-1 knock-out (SYNJ1 KO) p0 brains on the left and MEF on the right.*

## 4.5 PI3K/AKT/mTOR pathway

Because of triple knock-out of endophilin-A phosphorylation of p70S6 Kinase 1 (P70 S6K1) on Thr389 is significantly reduced (Figure 4.35) in mouse p0 brain what implies lower mTORC1 activity and restricted protein synthesis. Ribosomal protein S6 (S6) is phosphorylated by p70S6 Kinase 1 and, expectedly, decreased level of phosphorylated S6 was observed. Knock-out of endophilin-A leads to notably diminished phosphorylation of the serine/threonine kinase AKT (AKT) at S473 in mouse p0 brain what suggests decreased mTORC2 activity. Overall, triple knock-out of endophilin-A disturbs PI3K/AKT/mTOR pathway resulting in drastically decreased activities of AKT and mTOR, that is both its complexes mTORC1 and mTORC2. Protein levels were measured by *western* blot as described in *Methods*.

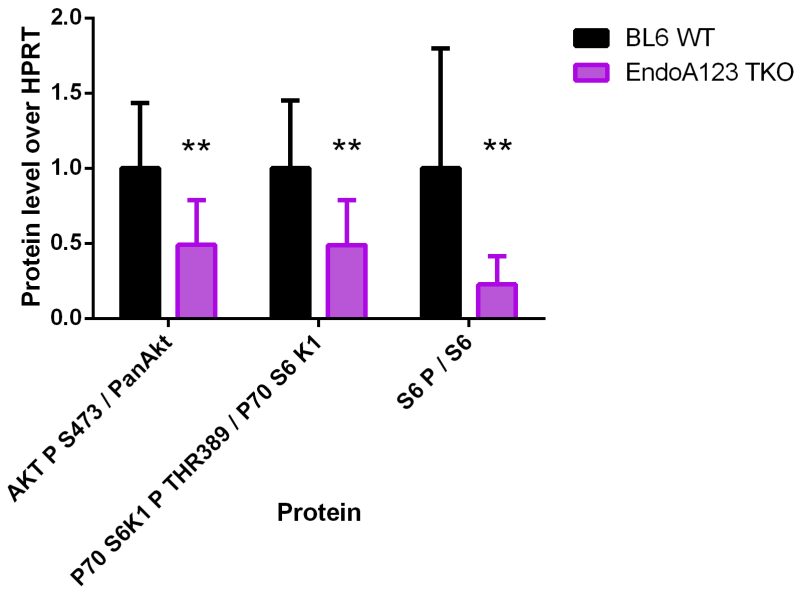


*Figure 4.35 Levels of proteins phosphorylated by mTORC1 or mTORC2 detected by western blot in C57BL/6J wild type (BL6 WT) and endophilin-A triple knock-out (EndoA123 TKO) p0 brains. ** $P \leq 0.01$ from T-test.*

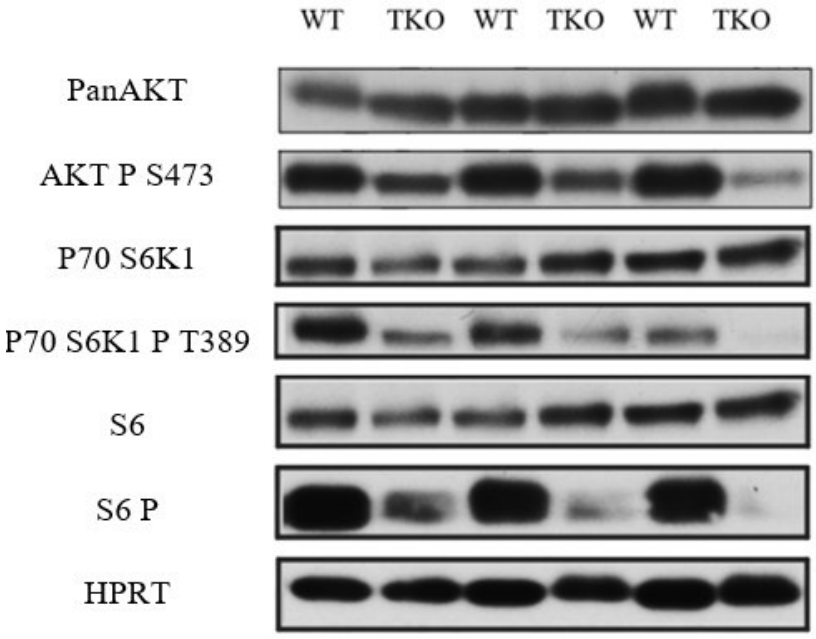


*Figure 4.36 Exemplary blots indicating levels of proteins phosphorylated by mTORC1 or mTORC2 in C57BL/6J wild type (BL6 WT) and endophilin-A triple knock-out (EndoA123 TKO) p0 brains.*

## 5 Discussion

Available literature suggests that there may be interdependence between mechanisms of endocytosis and the maintenance of mitochondrial structure and function since several proteins are necessary for proper mitochondrial work. Namely, ATPase EHD1, GTPases Dynamin-2 and dynamin-related protein-1 (Drp1) have very important role in mitochondrial fission. Endophilins B are closely related to endophilin-A and are essential for sequestration of the depolarized mitochondria and IMM protein degradation, while endophilin B1 is essential for preservation of mitochondrial morphology. Furthermore, inhibitors of clathrin mediated endocytosis disturb mitochondria: Endosidin9 and tyrosine kinase inhibitor tyrphostinA23 uncouple mitochondrial oxidative phosphorylation [1] [2] [3] [4].

This scientific work investigates impact of defective endocytosis due to knock-out of endophilin-A or synaptojanin-1 on mitochondrial function. Mitochondria are very important organelles of the eukaryotic cell. They are responsible for energy production in the form of ATP, synthesis of haeme and Fe-S clusters, and phospholipid and calcium buffering (Duchen, 2000). Mitochondria can also activate the intrinsic cell death pathway and induce apoptosis (Green and Reed, 1998). Statistical analysis of Next Generation Sequencing data implies that knock-out of endophilin-A or synaptojanin-1 results in a global downregulation of gene expression of mitochondrial proteins in newborn (p0) mouse brain.

In both endophilin-A triple knock-out and synaptojanin-1 knock-out MEF, reduced mitochondrial membrane potential was observed. Adequate membrane potential of the mitochondria is necessary for the sufficient ATP production and efficient transport. Impaired import leads to faulty mitochondrial function and shape as variety of mitochondrial proteins are encoded in the nucleus [31]. The inner mitochondrial membrane includes the respiratory chain and oxidative phosphorylation machineries, which produce ATP using oxygen consumption (Mitchell, 1961; Mitchell and Moyle, 1967). In endophilin-A triple knock-out and synaptojanin-1 knock-out MEF, the oxygen consumption rate is significantly decreased and can be elevated but not rescued by supplementation with pyruvate. Pyruvate is the eventual product of glycolysis and provides the first substrate for the tricarboxylic acid cycle in mitochondria [30]. The presented data, that is mostly reduced gene expression and altered levels of glycolytic enzymes in mouse p0 brains and MEF suggest that knock-out of endophilin-A or synaptojanin-1 slightly affects glycolysis. However, there is no consistent trend in levels of glycolytic enzymes that could be a reason of possible alterations in glycolytic activity and great decrease of oxygen consumption rate. This indicates that defect is not extrinsic, but intrinsic to mitochondria. Moreover, elevated superoxide levels were detected in endophilin-A triple knock-out MEF. Superoxide is the predominant among by-products of oxidative phosphorylation which are called reactive oxygen species. Typically, mitochondrial antioxidant defences convert the superoxide to hydrogen peroxide and then to water. In pathological conditions superoxide level might be excessively high for standard defences or they may be attenuated [29]. Overall, presented results indicate that knock-out of endophilin-A or synaptojanin-1 leads to mitochondrial malfunction that is more severe in case of endophilin-A triple knock-out.

Furthermore, raised lysosomal mass and decreased proteolytic activity were observed in endophilin-A triple knock-out and synaptojanin-1 knock-out MEF which are characteristic for lysosomal dysfunction. Mitochondria are constantly interacting with the rest of the cell; thus, mitochondrial insufficiency influence other organelles and perturbs their function and biogenesis. Part of the characteristic of mitochondrial diseases are functional and structural alterations of lysosomes and peroxisomes. On the other hand, mitochondrial flaws are observed in many peroxisomal and lysosomal diseases. It should be further studied if endophilin-A triple knock-out or synaptojanin-1 knock-out results in

mitochondrial dysfunction that causes lysosomal defects or in opposite, knock-out of these proteins may lead initially to lysosomal deficiency and mitochondrial malfunction in consequence [35].

Levels of iron in a body have to be maintained within exact boundaries to ensure proper cell function and lack of such control may affect whole organism. Shortage of iron results in cellular growth arrest and death. Defective endocytosis most likely debilitates iron trafficking and, in consequence, leads to functional iron deficiency which was detected in endophilin-A triple knock-out. It probably contributes to described above mitochondrial malfunction due to the fact that iron is an essential cofactor in numerous biological processes, such as oxygen transport, cellular respiration and mTORC1 function [38]. It should be verified how supplementation with iron, for example ferric citrate, affects mitochondrial function in endophilin-A triple knock-out and in BL6 wild type as a control.

Predictably, knock-out of endocytic proteins endophilin-A affects PI3K/AKT/mTOR pathway resulting in significantly reduced activities of AKT and mTOR, that is both its complexes mTORC1 and mTORC2. mTORC1 regulates the balance between anabolism and catabolism by enhancing production of proteins, lipids, nucleotides and inhibiting catabolic pathways like autophagy. MTORC1 boosts protein synthesis mainly through the phosphorylation of the two critical effectors: p70S6 Kinase 1 (S6K1) and eIF4E Binding Protein. S6K1 is directly phosphorylated by mTORC1 on its hydrophobic motif site (Thr389) and, later, phosphorylated and activated by PDK1 to, afterward, phosphorylate and activate several substrates that foster mRNA translation initiation. Due to knock-out of endophilin-A phosphorylation of S6K1 on Thr389 is significantly decreased in mouse p0 brain what suggests reduced mTORC1 activity and lowered protein synthesis. mTORC2 controls proliferation and survival mainly by phosphorylating various members of the AGC family of protein kinases. One of the critical functions of mTORC2 is the phosphorylation at residue S473 and consequent activation of Akt, which is most important effector of insulin/ PI3K signalling. Knock-out of endophilin-A results in notably diminished phosphorylation of AKT at S473 in mouse p0 brain what indicates lessened mTORC2 activity. Such aberrant activity may have various meaningful consequences because mTOR signalling is responsible for coordination of metabolism at both, the cellular and organismal level. Adequate mTOR activity is substantial for control of protein synthesis, autophagy and critical neurological processes like neural development [37].

After all, endophilin-A and synaptojanin-1 are necessary for appropriate mitochondrial and lysosomal function. Knock-out of endophilin-A leads to functional iron deficiency and significantly decreased activity of PI3K/AKT/mTOR pathway. It is recommended to investigate if endophilin-A or synaptojanin-1 have any particular role in mitochondrial function or all observed effects result only from impaired endocytosis.

# 6 Conclusions

Links between endocytic process and the maintenance of mitochondrial structure and function were previously implied since several endocytic proteins are necessary for proper mitochondrial function as well. The data presented here confirms that impaired endocytosis, due to knock-out of endophilin-A or synaptojanin-1, affects mitochondrial function. Statistical analysis of Next Generation Sequencing data implies that knock-out of endophilin-A or synaptojanin-1 results in a downregulation of gene expression of mitochondrial proteins. Mitochondrial malfunction was recognized basing on following features: decreased mitochondrial membrane potential, diminished oxygen consumption rate, slightly affected glycolysis and raised reactive oxygen species production. Additionally, elevated lysosomal mass and reduced proteolytic activity were detected which are characteristic for lysosomal defects.

Interestingly, striking functional iron deficiency was identified in endophilin-A triple knock-out which probably contributes to observed mitochondrial malfunction as iron is an essential cofactor in several biological processes, such as oxygen transport, cellular respiration and mTORC1 function. On the other hand, mTOR pathway regulates iron metabolism and homeostasis. Expectedly, PI3K/AKT/mTOR pathway is notably disturbed by knock-out of endophilin-A, particularly activities of AKT and mTOR, that is both its complexes mTORC1 and MTORC2, are significantly decreased. Such reduced activity may result in various severe consequences since mTOR signalling controls metabolism at both, the cellular and organismal level. Accurate mTOR activity is also required for regulation of protein synthesis, autophagy and essential neurological processes, such as neural development.

It is recommended to verify whether endophilin-A triple knock-out or synaptojanin-1 knock-out leads to mitochondrial malfunction and in consequence lysosomal deficiencies. Alternatively, knock-out of these proteins may cause lysosomal defects primarily that then result in mitochondrial dysfunction.

In essence, endophilin-A and synaptojanin-1 are needed for normal mitochondrial and lysosomal functions. In addition, lack of endophilin-A results in functional iron deficiency and significantly reduced activity of PI3K/AKT/mTOR pathway.

## 7 References

1. T. Farmer, J. B. Reinecke (2017), Control of Mitochondrial Homeostasis by Endocytic Regulatory Proteins, Journal of Cell Science 130; doi:10.1242/jcs.204537.
2. Y. Takahashi, Ch. L. Meyerkord, (2009. July), Bif-1/Endophilin B1: a candidate for crescent driving force in Autophagy, *Cell Death & Differentiation, 16(7): 947-955*. doi: 10.1038/cdd.2009.19.
3. Y. H. Wang et al. (2016), Endophilin B2 promotes inner mitochondrial membrane degradation by forming heterodimers with Endophilin B1 during mitophagy, *Scientific Reports 6, 25153;* doi: 10.1038/srep25153.
4. Dejonhe W. et al. (2016), Mitochondrial uncouplers inhibit clathrin-mediated endocytosis largely through cytoplasmic acidification, Nat. Common. 7:11710, doi: 10.1038/ncomms11710.
5. Hilleman et al. (2013), Massive endocytosis triggered by surface membrane palmitoylation under mitochondrial control in BHK fibroblasts, eLife 2013;2:e01293, doi: 10.7554/eLife.01293L.
6. D. Osellame, M. R. Duchen (2014), Quality control gone wrong: mitochondria. lysosomal storage disorders and neurodegeneration, *British Journal of Pharmacology*, 171, 1958-1972.
7. J. L. Goldstein, R. G. W. Anderson & M. S. Brown (1979. June 21), Coated pits, coated vesicles, and receptor-mediated endocytosis, *Nature Val. 279*.
8. Endocytosis: receptor-mediated endocytosis. *Art. Britannica Online for Kids. Web. 8 Jan. 2017.*
9. K. Aoyagi et al (2015, August), A Gain-of-Function Mutation in NALCN in a Child with Intellectual Disability, Ataxia, and Arthrogryposis, *Human Mutation 36. issn: 1098-1004*, 753–757.
10. L. Calò et al., Interaction between Ephrins/Eph Receptors and Excitatory Amino Acid Receptors: Possible Relevance in the Regulation of Synaptic Plasticity and in the Pathophysiology of Neuronal Degeneration, *Journal of Neurochemistry 98, issn: 00223*, 1–10.
11. K. Chen (2015, October), Mutational Analysis of SYNJ1 Gene (PARK20) in Parkinson's Disease in a Taiwanese Popµlation, *Neurobiology of Aging 36, 2905.e7-8, issn: 1558-1497*.
12. S. Connert, (2006, April 19), SH3P7/mAbp1 Deficiency Leads to Tissue and Behavioral Abnormalities, *The EMBO Journal, 25(8)*, 1611–1622, doi:10.1038/sj.emboj.7601053
13. D. A. Dyment, (2015, February), Homozygous Nonsense Mutation in SYNJ1 Associated with Intractable Epilepsy and Tau Pathology, *Neurobiology of Aging*, 36, 1222.e1–1222.e5.
14. F. C. Herrera (2009, June), Synaptojanin-1 Plays a Key Role in Astrogliogenesis: Possible Relevance for Down's Syndrome, *Cell Death & Differentiation*(16), 910-920, doi:10.1038/cdd.2009.24
15. V. Drouet, S. Lesage (2014), Synaptojanin 1 Mutation in Parkinson's Disease Brings Further Insight into the Neuropathological Mechanisms, *BioMed Research International*, OCLC: 5693597125, issn: 2314-6133.
16. C. W. So, M. H. Sham (2000, June), Expression and Protein-Binding Studies of the EEN Gene Family, New Interacting Partners for Dynamin, Synaptojanin and Huntingtin Proteins, *Biochemical Journal 348, 447–458, issn: 0264-6021*.

17. S. V. Voronov, (2008, August), Synaptojanin 1-Linked Phosphoinositide Dyshomeostasis and Cognitive Deficits in Mouse Models of Down's Syndrome, *en. PNAS 105, 9415–9420, issn: 0027-8424, 1091-6490*.
18. L. Zhu et al (2015, September), Phospholipid Dysregulation Contributes to ApoE4-Associated Cognitive Deficits in Alzheimer's Disease Pathogenesis, *en. PNAS 112, 11965–11970, issn: 0027-8424. 1091-6490*.
19. K. Soda, D. M. Balkin (2012, December), Role of dynamin, synaptojanin, and endophilin in podocyte foot processes, *The Journal of Clinical Investigation, Volume 122, Number 12.*
20. M. Quadri, M. Fang (2013, June), Mutation in the SYNJ1 Gene Associated with Autosomal Recessive, Early-Onset Parkinsonism, Wiley Online Library, doi: 10.1002/humu.22373.
21. Cao. M., Milosevic. I., Giovedi. S. & De Camilli. P. (2014), Upregulation of Parkin in Endophilin Mutant Mice, *The Journal of Neuroscience*, *34*(49), 16544–16549, doi: 10.1523/JNEUROSCI.1710-14.201
22. Kuijpers, Marijn et al. (2016, November), Autophagosome Formation by Endophilin Keeps Synapses in Shape, Neuron, Volume 92, Issue 4, 675 - 677.
23. Milosevic et al. (2011, November), Recruitment of Endophilin to Clathrin-Coated Pit Necks Is Required for Efficient Vesicle Uncoating after Fission, Neuron 72, 587–601, doi: 10.1016/j.neuron.2011.08.029
24. S. B. Martin, A. L. S. Dowling (2014), Synaptophysin and synaptojanin-1 in Down syndrome are differentially affected by Alzheimer disease, *Journal of Alzheimer's Disease, 42(3), 767–775*, doi: 10.3233/JAD-140795.
25. Murdoch et al. (2016. October), Cell Reports 17, 1071–1086.
26. R.A. Gottlieb, D. Bernstein (2016), Mitochondrial remodelling: Rearranging, recycling, and reprogramming, *Cell Calcium*.
27. P. J. Fernandez-Marcos, Auwerx J. (2011), Regulation of PGC-1a, a nodal regulator of mitochondrial biogenesis, *The American Journal of Clinical Nutrition 2011;93(suppl):884S–90S*, doi: 10.3945/ajcn.110.001917.
28. Vartak, R., Porras, C.AM. & Bai, Y. Protein Cell (2013) 4: 582. doi: 10.1007/s13238-013-3032-y
29. Zorov, D. B., Juhaszova, M., & Sollott, S. J. (2014), Mitochondrial Reactive Oxygen Species (ROS) and ROS-Induced ROS Release, Physiological Reviews, 94(3), 909–950, doi: 10.1152/physrev.00026.2013.
30. Li. X., Gu. J., & Zhou. Q. (2015), Review of aerobic glycolysis and its key enzymes – new targets for lung cancer therapy, Thoracic Cancer, 6(1), 17–24, doi: 10.1111/1759-7714.12148.
31. R. Ventura-Clapier, A. Garnier, V. Veksler (2008), Transcriptional control of mitochondrial biogenesis: the central role of PGC-1a, *Cardiovascular Research 79. 208-217,* doi: 10.1093/cvr/cvn098.
32. C.V. Diogo et al. (2017), Mitochondrial adventures at the organelle society, Biochemical and Biophysical Research Communications, 1-7, doi: 10.1016/j.bbrc.2017.04.124
33. Y. Xie, B. Zhou (2015), Endolysosomal deficits augment mitochondria pathology in spinal motor neurons of asymptomatic fALS mice, Neuron 87, 355e370.
34. J. Kong, Z. Xu. (1998), Massive mitochondrial degeneration in motor neurons triggers the onset of amyotrophic lateral sclerosis in mice expressing a mutant SOD1, J. Neurosci. 18 3241e3250.

35. L. Fernandez-Mosquera, C.V. Diogo (2017), Acute and chronic mitochondrial respiratory chain deficiency differentially regulate lysosomal biogenesis, Sci. Rep, 7, 45076.
36. N. Raimundo, L. Fernández-Mosquera, (2016, August), Mechanisms of communication between mitochondria and lysosomes, The International Journal of Biochemistry & Cell Biology 79, 345-349, doi: 10.1016/j.biocel.2016.08.020
37. Saxton et al. (2017, March), mTOR Signalling in Growth, Metabolism, and Disease, Cell, Volume 168, Issue 6, 960-976. doi: 10.1016/j.cell.2017.02.004.
38. Peng G, Na W. (2014), The Mammalian Target of Rapamycin Coordinates Iron Metabolism with Iron-sulfur Cluster Assembly Enzyme and Tristetraprolin, Nutrition, doi: 10.1016/j.nut.2013.12.016.
39. Cremona, Ottavio et al. (1999), Essential Role of Phosphoinositide Metabolism in Synaptic Vesicle Recycling, Cell, Volume 99, Issue 2, 179 - 188,
40. H. Bouabe, K. Okkenhaug (2013), Gene Targeting in Mice: a Review, Methods Mol Biol., 1064: 315–336, doi:10.1007/978-1-62703-601-6_23.